5-2016

Design and Manufacture of a Biodegradable Ureteral Stent

James Hyde
Clemson University, jhyde@g.clemson.edu

Follow this and additional works at: https://tigerprints.clemson.edu/all_theses

DESIGN AND MANUFACTURE OF A BIODEGRADABLE URETERAL STENT

A Thesis
Presented to
the Graduate School of
Clemson University

In Partial Fulfillment
of the Requirements for the Degree
Master of Science
Bioengineering

by
James Hyde
May 2016

Accepted by:
Dr. Jiro Nagatomi, Committee Chair
Dr. O. Thompson Mefford
Dr. John Desjardins

ABSTRACT

Approximately 92,000 ureteral stents are implanted every year to maintain urine flow after treatment of kidney stones, kidney transplants, and urinary incontinence. However, current ureteral stents have several downsides that include encrustation, urgency due to the proximal curl pressing on the bladder, patient pain from inflexible stents, and most importantly, the need for a follow up removal surgery. To address many of these current issues, a novel biodegradable stent was designed, fabricated, and characterized in the present studies. The innovative stent design features the use of biodegradable, FDA approved polydioxanone polymer material that was aimed to reduce encrustation and eliminate the need for a removal surgery. Additionally, the stent's novel coiled shape is intended to provide flexibility and anchor into the ureter. By eliminating the clinically conventional "double J" anchors, this could prevent the issue of the proximal anchor pressing on the bladder, remove the risk of encrustation on the distal anchor, and provide for better patient comfort by creating a more axially flexible stent. The novel stent was fabricated by winding a PDO suture around a mandrel and annealing at 100 °C. This annealing step increased the stiffness of the polymer as determined by cantilever bend testing. The source of this stiffness increase was determined to be due to an increase in crystallinity as verified by Differential Scanning Calorimetry and Wide Angle X-Ray Scattering. The results of custom testing in the present study also provided evidence that the stent exhibits adequate anchor strength and radial strength to maintain patency, which would allow standard ureteral flow conditions. Finally, an in vitro experiment demonstrated that the stent degrades in four weeks under normal

physiological conditions, which is believed to be the ideal degradation time for the majority of ureteral stent applications. The results of this thesis provide strong supporting evidence that the proposed stent design has the ability to improve patient outcomes by addressing the drawbacks of current stent technology. However, further characterization efforts using animal models will be necessary to assure the safety and efficacy of this technology before it is ready for clinical use.

DEDICATION

This thesis is dedicated to my loving parents, Kevin and Cindy Hyde, who have done more for me than words can express. I would also like to dedicate this thesis to Harleigh Warner who inspires me to be a better person every day.

ACKNOWLEDGMENTS

I wish to thank my advisor, Dr. Jiro Nagatomi, for his guidance and endless patience with me. I would also like to thank Dr. Thompson Mefford for his advice in all things material science and Dr. John Desjardins for his great assistance in developing a test plan for a medical device.

Thanks also to Christian Macks for the time during his undergrad that he spent with me at nonstandard hours in lab, setting up Arduino programs and collecting ureters from an abattoir at 5 am on a holiday. I would also like to thank Snow Creek Meat Processing plant for their help in tissue collection.

Lastly, I want to thank Clemson University and the entire Department of Bioengineering for providing me this opportunity to further my education.

TABLE OF CONTENTS

TABLE OF CONTENTS (continued)

LIST OF TABLES

LIST OF FIGURES

LIST OF FIGURES (Continued)

1. LITERATURE REVIEW

1.1 Clinical Motivation

To maintain patency to sustain a steady flow of urine from the kidney to the bladder, ureteral stents are implanted after nearly every nephrological procedure including treatment for urinary incontinence, kidney stones, and renal transplants. [1], [2], [3] Ureteral stents have had a significant impact in the field of urology, turning many procedures that would have required overnight stays in the hospital into outpatient procedures [4]. Despite their popularity, several downsides to using current ureteral stent technology exist. First, when a stent is implanted for any length of time, encrustation of the device can occur.[5], [6], [7] Most significantly, ureteral stents always require a second procedure to be removed. Though time varies based on the procedure, it is rare for a stent to be implanted longer than 90 days. [8], [9], [10] This removal procedure is both a loss of time for the urologist and an additional expense for the patient.   To date, however, these problems are yet to be solved by existing stent technologies.

1.2 Anatomy of the Urinary System

The urinary system consists of the kidneys, ureters, bladder, and urethra and its main function is to remove waste (e.g., uric acid, creatinine, ammonium, ions, sulphates, phosphates, and oxalates) [11] from the blood stream and convert it into urine. The urine travels down the ureters into the bladder where it is stored. Voiding of the urine through

the urethra takes place by coordinated relaxation of the external urethral sphincter and contraction of the bladder smooth muscle forcing the urine out of the body. [12]
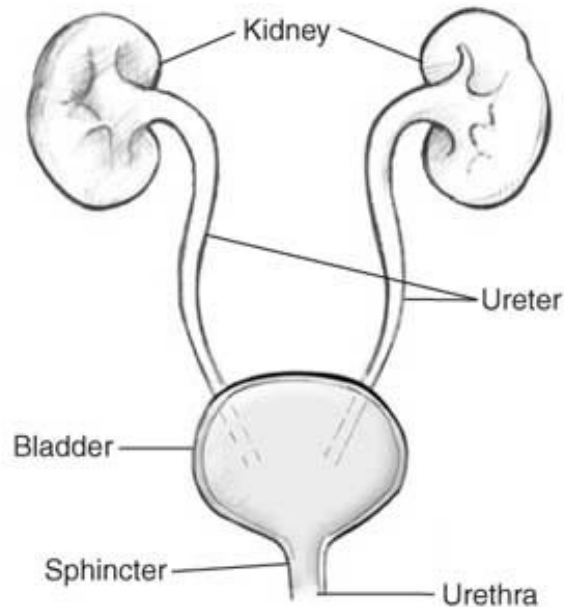
Figure 1-1 Urinary System

[13]

1.2.1 Kidney

The kidneys (Fig. 1-1) are bean shaped organs that filter waste out of the blood by 1 million tiny units called nephrons. [14] Within each nephron is the glomerulus with specialized structures called fenestrae that selectively allow small molecules to pass through and retain larger substances like red blood cells in the blood. This filtrate is combined with water secreted by the kidney to produce urine. The urine is transported through a tubule through the inner part of the kidney into the collecting duct. Urine is then transported by the ureter to the bladder. [12]

2
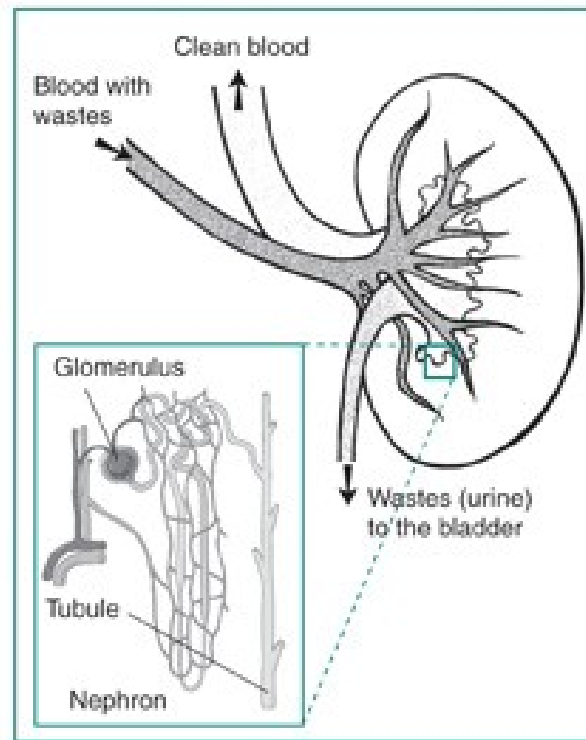
Figure 1-2 Nephron

[15]

1.2.2 Ureters

The ureters are roughly 25 cm in length and allow transport of urine from the kidney to the bladder via peristalsis. The wall of the ureter is composed of three layers, the mucosa, muscularis, and adventitia. Unlike other transport tubules such as the GI tract, the ureter lacks the connective tissue layer known as the submucosa.

The innermost, mucosa layer is further divided into transitional epithelium, which prevents urine absorption, and the lamina propria, a relatively thick layer of connective tissue. The mucosa typically exhibits a folded morphology. However, as peristaltic

waves travel the ureter, the folds can stretch which increases the diameter of the ureter dramatically. [12] The muscularis responsible for peristaltic motion is composed of two bands of smooth muscle orthogonally oriented in longitudinal and circular directions. This muscle contracts in a wave like motion to form boluses of urine that move along the ureter in the inferior direction. It has been reported that the pressure generated by the peristalsis can be as high as 1.9 kgf/cm^2 [16] The outermost adventitia layer is composed of aereolar connective tissue and its primary purpose is to anchor the ureter to the posterior abdominal wall.
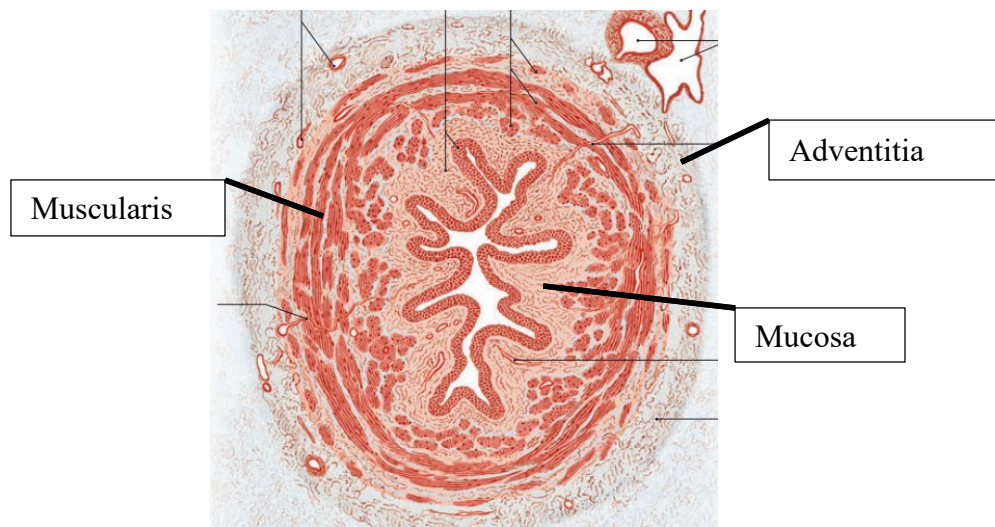
Figure 1-3 Histology of the Ureter

(Adapted from [17])

Blood supply to the ureter is provided from the branch of the nearest artery (e.g., renal arteries, aorta, common iliac, or internal iliac arteries) and drainage is from companion veins.
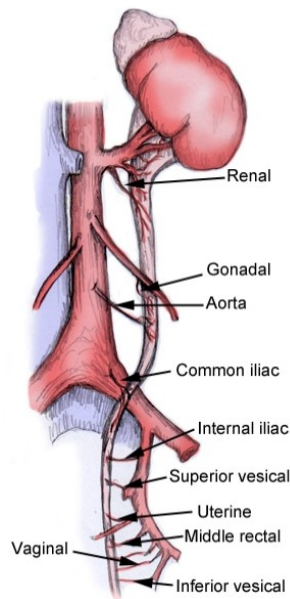
Figure 1-4 Vascularization of the ureter

[18]

The superior region of the ureter is innervated by parasympathetic fibers from the Central Nervous System (CNX) via the dorsal vagus nerve, while the inferior region is innervated by the pelvic splanchnic nerves. While not known definitively, it is believed that this modulates intrinsic pacemaker cells, which cause the regular peristaltic action. [19]

It has been observed that the ureter has three physiologic narrowings. First, where the ureter connects to the kidney, is called the ureteropelvic junction. Second, where it crosses over the iliac vessel. Finally, where it connects to the bladder called the ureterovesical junction. The ureteropelvic junction and ureterovesical junction are the location where stones are most likely to be trapped. [20] These three narrowings also limit retrograde instrumentation such as placement of a ureteral stent.

1.2.3 Urinary Bladder

The bladder is an organ whose purpose is storage and periodic voiding of urine. The bladder can contain on average 350 mL of urine before urgency to urinate is felt, but as much as 700 mL can be retained in adult humans. [21] Due to its folded rugae and high elastin content the bladder is highly distendable. [22], [23], [24] During storage of urine, continence is maintained by the external uretheral sphincter. [12]

Backflow into the ureter is prevented by the special anatomical structure of the vesicoureteral junction. Instead of connecting perpendicular to the bladder wall, the ureter enters the bladder diagonally and runs 1.2-2.5 centimeters along the bladder wall (Figure 1-5). [17] When the bladder is filled this segment flattens, thus preventing backflow of the urine into the ureter.
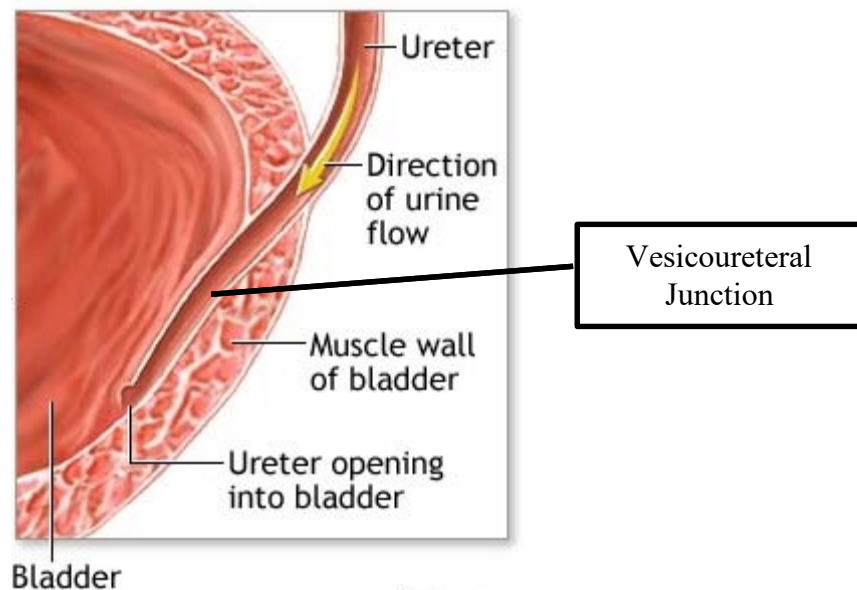
Figure 1-5 Vesicoureteral Junction

(Adapted from [25])

1.3 Ureteral Stents

Ureteral stents are devices that are implanted to physically hold open the ureter allowing urine to flow. Indications that determine when to use a ureteral stent can be broadly organized under five main classifications are: 1) Relief of a cancerous obstruction; 2) Adjunct to stone therapy; 3) Perioperative placement; 4) Management of urine leak; and 5) Relief of ureteral stricture. The most typical indication for stent use is as part of kidney stone treatment. [26], [27], [28]

It is worth noting that the terminology for ureteral stents has changed over the years. Until the 1950s the terms tube, catheter, and retention catheter were adequate to describe procedures in urology. [29] The first publications on ureteral stents used the term "splint" perhaps because it was used to immobilize the ureter in a fashion similar to a leg splint. Researchers often retroactively refer to what was called "splints" as "stents". [29], [30] Additionally, there is some confusion between the term "ureteric" and "ureteral". The author has found no differentiation between these two terms, though it appears that "ureteral" is the most common usage. For the purpose of this paper all descriptions will classified as "ureteral stents".

The first stent described in literature in 1952 was little more than a silicone tube. [30] While it provided adequate drainage, it frequently migrated into the bladder. [31] In 1967, ureter specific stent was designed by Gibbons, who successfully created an anchor to hold the stent in place in the ureter. The Gibbons stent was barbed on the exterior to keep it from moving down the ureter and had a "C" shaped bend at the

proximal end to prevent the stent from moving up the ureter. While initially popular the Gibbons stent is no longer on the market due to difficulty with insertion. [32], [33]

Figure 1-6 Gibbons Stent

[32]

It wasn't until the introduction of the double-pigtail and double-J stent configuration in 1978, that stents were regularly used without experiencing major problems. [34] Today, numerous materials, coatings, and stent designs have proven to be more effective in restoring regular flow of urine into the bladder. The two most common materials used in stent production today are silicone and polyurethane.
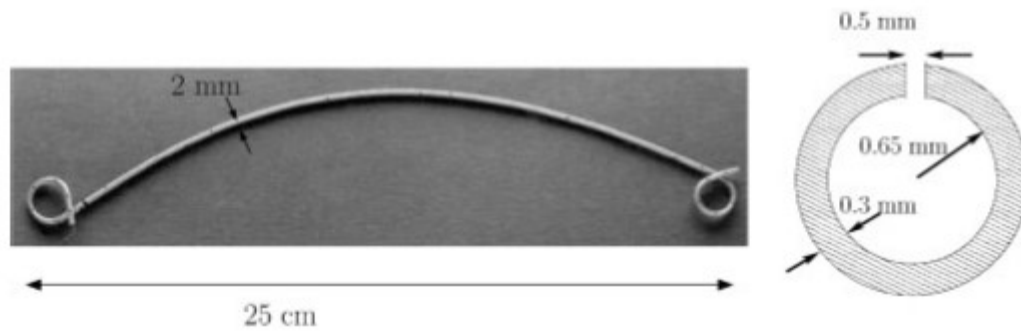
Figure 1-7 (a) Ureteral Stent with double pig tail anchor (b) Cross-section with drainage hole

[7]

1.3.2 Complications of Ureteral Stents

As ureteral stents usage increases, so too has the incidence of related complications. While stents are generally considered safe they are not without risk. Complications pertaining to ureteral stents can be broadly separated into seven categories.

1.3.2.1 Irritative Bladder Symptoms

By far the most common side effect of ureteral stenting is irritative bladder symptoms, which occurs in up to 80% of patients. [35] Irritative bladder syndrome is an inclusive term for voiding symptoms, flank and suprapubic pain, incontinence and hematuria. It is viewed as a manageable side effect and is typically treated with pain prescription. [3]

1.3.2.2 Urinary Tract Infection

When a stent is introduced to the normally sterile ureter, the risk of infection in the

9

urinary tract increases. After implantation, proteins rapidly adsorb to the stent surface,

which enable deposition of minerals and other urine components as well as attachment of

bacteria. The most common bacteria seen in urinary tract infections (UTIs) are

Escherichia coli (E coli), *Staphylococcus* and *Pseudomona.* [10] In most patients,

antibiotic prophylaxis is performed, typically in a single dose immediately before the

stenting procedure.

1.3.2.3 Inadequate Relief of Obstruction

Under various situations a stent may not restore urine flow as intended. For

example, loss of flow within hours of insertion may be a result of blood clotting or debris

from a severe infection, both of which are extremely dangerous and require immediate

care. [36] Occlusion can also be a result of extrinsic pressure. Stents of smaller

diameter can be collapsed by pressure from a tumor or stricture. [13]

1.3.2.4 Ureteral Erosion or Fistulization

Ureteral erosion is the most dangerous of all the complications associated with

stents. Although the etiologies are complex and difficult to diagnose, the dominant

symptom of erosion is gross Hematuria. However, by that point erosion has already

taken place. [38] Factors that increase the likelihood of erosion are prolonged stent use,

prior pelvic surgery, cancer and extensive irradiation. The presence of a pulsating

vascular structure, (normal vessel, graft, or aneurysm) to a rigid stent has also been

associated with erosion. [38], [32]

1.3.2.5 Malposition and Migration

Malposition of the stent may result from human errors during placement although urologists are recommended to use fluoroscopy. Stents made of stiffer material may accidentally pierce through the ureter wall resulting in an urinoma or hematoma [32]. The stent that is not pushed all the way to the kidney may cause the anchor to stay straightened in the ureter instead of curled in the kidney. The force of self-curling can bury the stent anchor into the wall of the ureter making removal difficult.

Migration of the stent from its placement origin can happen both superiorly into the kidney and inferiorly into the bladder. Most commonly the stent migrates into the bladder due to peristaltic motion from the ureter and pressure from urine creation in the kidney. Instances of this complication have increased recently, likely due to the new hydrophilic coatings that reduce the friction of the stent. [32]

1.3.2.6 Encrustation

All stents elicit different forms and degrees of encrustation after insertion. The presence of the stent provides a substrate for the deposition of minerals including calcium oxalate, struvite, apatite, and uric acid along with organic macromolecules. While all these can be present, calcium oxalate typically makes up the largest portion of encrustation. [5] Risk factors for encrustation include stone disease, urinary sepsis, chemotherapy, pregnancy, chronic renal failure, metabolic or hormonal abnormalities, and the most important being the indwelling time. [27] The most common location of encrustation is the proximal end at the anchor that sits in the kidney. This location is

more prone because the concentration of solutes is higher in the kidney. It has also been suggested that peristalsis may have a cleaning effect on the body of the stent, and, thus, encrustation is rare. [6], [27]

1.3.2.7 Urine Reflux During Voiding

Due to the proximal anchor of the ureteral stent sitting in the bladder, the vesicoureteral valve is forced open by the stent body. During voiding, this forces urine up the ureter and into the kidney. This can cause pain and increases the risk of infection. [4][7]

1.3.2.8 Stent Fracture

Stent fracture is becoming increasingly less frequent as materials for stents have improved over time. However, there is still a risk of fracture. Fracture typically occurs at the drainage holes (also called fenestrations). [36]

1.3.3 Materials for Ureteral Stents

Many materials have been proposed for use in ureteral stents. The first-generation of stents were made of silicone. [39] While still considered the gold standard, silicone is rarely used in ureteral stents without a coating due to its high coefficient of friction. [40] After silicone, polyethylene was introduced as the material for ureteral stents. Due to the high risk of fracturing, however, polyethylene is not as widely used today. Finally,

polyurethane was introduced onto the market. While rarely used alone it has been prized

for its ease of coating and modification. [39], [41] Metal stents also exist in a small

niche for extremely long indwelling times and for very tight strictures.

1.3.3.1 Polymers for Ureteral Stents

Many different polymers have been proposed for use in ureteral stents. While

much research has been done, the two main stent materials remain silicone and

polyurethane. However, within the context of these two materials many modifications

have been performed.   Coatings have been added to reduce friction for ease of

implantation and reduce encrustation. [42] Substrate modifications have been performed

to improve material properties such as stiffness and hydrophilicity. [39]

1.3.3.1.1 Polyurethanes

Polyurethane (PU) is a polymer composed of an organic group attached via

carbamate groups ($-NHCO_2-$). Although, it has long been used a stent material with

many different kinds currently on the market, polyurethane has been shown to be more

prone to encrustation than silicone. [43]

1.3.3.1.2 Tecoflex

Tecoflex is an aliphatic PU blended with barium sulfate to provide a high

radiopacity. Tecoflex is a thermoset PU and is used in stents because of its ability to

soften when warmed by the body after stenting. This allows it to be rigid for insertion

but more flexible after insertion for better patient comfort. Tecoflex stents are produced by Gyrus ACMI. [44]

1.3.3.1.3 Hydrothane

Hydrothane is a polytetramethylene glycol based alphatic PU produced by Cardiotech International. The addition of the glycol subunits increases the polymers' hydrophilicity. When used for stents, hydrothane can be processed without aromatic groups. This lack of aromatic groups increases biological inertness by reducing generation of dispersion (van der Waals) forces between the polymer and the proteins found in urine. [45], [46]

1.3.3.1.4 ChronoFlex

Also produced by Cardiotech International, Chronoflex was developed to be a more durable PU and studies have shown that it exhibits less environmental stress cracking than other PUs. [47] This polymer had more hydrophobic properties which suggests it forms a stable conditioning layer, thus preventing encrustation. [48]

1.3.3.1.5 Percuflex

Produced by Boston Scientific, this polymer is a proprietary olefinic block copolymer and is another thermosetting PU. Percuflex softens in the body and has better physical properties than PU. However, encrustation is similar to standard PU. Because

of the softening affect, these stents are not used in cases of stricture due to extrinsic obstruction because they are easily compressed. [43]

1.3.3.1.6 Aquavene

Aquavene is produced by Menlo Care Inc. and is a polyurethane blended with polyethylene oxide. When placed in water, it swells increasing in size, but maintaining strength. Aquavene is harder in dry conditions and softens rapidly when hydrated which aids in implantion and patient comfort. [49]

1.3.3.1.7 Sof-flex

Sof-flex is a proprietary polymer developed by Cook Medical that lists polyurethane as its primary ingredient. It has been used extensively in ureteral stents. It boasts a very small coefficient of friction because its hydrophilic properties hold water to its surface. Studies have shown low biofilm formation but increased encrustation of calcium carbonate. [39]

1.3.3.1.8 Silicone

Silicone is the "gold standard" material for ureteral stents and is composed of alternating silicone and oxygen atoms. Due to its uniform surface, it is less prone to encrustation than PU and hydrogel-coated PU. Because of its inertness, it is ideal for long implantation times. However, silicone is almost never used without some sort of surface coating because its high-coefficient of friction makes implantation difficult. [43]

1.3.3.1.9 Silitek

Silitek, produced by ACMI, is a proprietary polyester copolymer made to replace silicone. It is firm and has a high radial stiffness to resist compression. Studies have shown that it has an encrustation profile similar to silicone. It has relatively weak coil retention strength which may make it more likely to migrate. [50]

1.3.3.1.10 C-Flex

C-flex, produced by is a polymer made up of styrene/ethylene-butylene/styrene block copolymers. It has thermoplastic properties and has been clinically used in stents. It is comparatively weak when compared to other stent types but is adequate for typical stenting. [50] Uncoated C-flex stents are sold by Cook medical while Boston Scientific sells a hydrogel coated stent that lowers its coefficient of friction. However, it has been shown that the hydrogel coated stents are more prone to encrustation. [43]

1.3.3.2 Coatings of Ureteral Stents

Various stent coatings have been explored for prevention of encrustation and bacterial adhesion or for easier implantation by decreasing surface friction. In addition, many studies have investigated the release of antibiotics and other chemicals from hydrogel coating on stent surface.

1.3.3.2.1 Hyaluronic Acid (HA)

HA is a glycosaminoglycan that inhibits the nucleation, growth, and aggregation of salts. [51] For this reason, it has been explored as an anti-encrustation coating. Plasma treatment has been used to covalently bond HA to polyurethane stents. An *in vitro* study showed that HA coated stents have a lower rate of encrustation than silicone stents. [52]

1.3.3.2.2 Heparin

Heparin is a highly sulfated glycosaminoglycan that is known most as an anticoagulant. Heparin has the highest negative charge density of all known biological molecules. [53]   Heparin coated stents have been shown to prevent biofilm formation in human pilot studies over a 6-8 week time period. This is attributed to heparin's electronegativity repelling proteins and microorganisms. [54]

Heparin can be adsorbed to the stent surface, incorporated into the stent material, or covalently bonded to the surface. Because of the risk of leaching and limited effectiveness with the first two approaches, covalent bonding is considered to be the most effective method. [55]

1.3.3.2.3 Polyvinylpyrrolidone (PVP)

PVP is a water absorbing polymer used as a coating for ureteral stents because of its excellent wetting properties. PVP provides a smooth, soft, water coating that minimizes difficulties during insertion. Adherence of bacteria and encrustation were

found to be less on PVP coated PU than uncoated PU because the water layer prevented bacterial adhesion. [56]

1.3.3.3 Metal

Metal stents are not used for routine stenting. However, metallic stents are used for instances when longer indwelling times are required. [57] Metallic stents are also much cheaper to manufacture. A 2010 study was performed in which 15 metal stents were placed in 13 patients to manage obstruction. Their health care costs were tracked for almost two years and then compared to national averages. It was found that the annual cost of metallic stenting was $11,183 while the average yearly costs for polymeric stents were $23,999. From this small sample it appears that metallic stents are an excellent cost saving measure. [58]

There have been a variety of metals explored in the context of ureteral stents. A self-expandable polytetrafluoroethylene-covered nitinol stent has been successfully used to manage strictures. In 2003 29 PTFE covered nitinol stents were implanted. The stent did not encrust and the PTFE covering greatly prevented hyperplasia. However, it had about a 22% migration rate which may explain why it has not seen clinical use since then. [59]

1.3.3.4 Biodegradable Polymers for Ureteral Stent Applications

Although no ureteral stents made entirely of biodegradable polymers are currently available on the market these polymers have gained interest due to their resistance to encrustation and the elimination of a stent removal procedure. [60] Following are

examples of the polymers that have been studied within this scope.

1.3.3.4.1 Polylactic Acid (PLA)

PLA (or polylactide) is a thermoplastic biodegradable aliphatic polyester, which can be processed into a fiber or into a film. [61] Due to the chiral nature of lactic acid, PLA can be further subdivided based on the D or L isomer, changing the naming convention to PLLA or PDLA. [62]

Lumiaho et al. explored self-expanding Poly-L-D-lactide as a material to fabricate a ureteral stent in a 2009 study. [63] Briefly, PLA was mixed with 20 wt% barium sulfide and extruded to create a fiber with 0.35mm in diameter. The fiber was then wrapped around a mandrel to create what the author calls a double helix structure with final inner and outer diameters of 1.3mm and 0.6mm, respectively. Following gamma sterilization, the PLA stents and control, 3.8F Double-J C-Flex® stents, were implanted in 6 dogs each. Although the PLA stent provided adequate renal output, fragments of the stent remained imbedded in the ureter after 12 weeks. [63] For this reason, in the subsequent studies the author switched from PLA to Poly Glycolic Acid. [64]

In a separate study, Gang et al. also explored the use of PLA as a ureteral stent material, with a special emphasis on relieving hydronephrosis caused by war injury. [65] Briefly, 50mm long stent segments were constructed by forming 50:50 PLLA/PDLA into a fiber and winding into a helical shape with 0.8mm and 1.4 mm inner and outer diameters, respectively. In vitro testing demonstrated that the stent took 10 weeks to degrade in synthetic urine. An *in vivo* canine model study demonstrated that the material

did not start degrading until day 80, and by day 120 only a few fragments were retained in the ureter. When injured unstented ureters, and injured stented ureters with the novel PLA stent were compared, it was found that the stents did improve urine flow. [65]

1.3.3.4.2 Polyglycolide (PGA)

PGA (Polyglycolide) has been shown degrade slowly into irregular sized fragments. Since PGA is brittle and mechanically inadequate, it has been used as a block copolymer with other biodegradable polymers for ureteral stent applications.

In a 2011 study, Lumiaho et al. would PLGA wire over a mandrel to fabricate a 40mm long stent with 4mm outer diameter. [63] Owing to its viscoelastic memory, the stent could expand in diameter up to 40% when heated from room temperature to body temperature.

An animal study on 8 pigs was performed to compare PLGA stents to the common double J stent. A small cystotomy was performed on both ureters and the left ureter was stented with PLGA stent segments while the right ureter was stented with double J stents. The type of double J stent material was not reported. After 4 weeks, 6 of the 8 PLGA stents showed no reflux, while 2 showed minor reflux. All double J stents showed some type of reflux. [63]

1.3.3.4.3 Temporary Ureteral Drainage Stent by Boston Scientific

In 2002, Boston Scientific began trial of a biodegradable stent with a product name, Temporary Ureteral Drainage Stent (TUDS). It was made of a proprietary alginate based

polymeric material that was designed to last 48 hours before being fully degraded in the body. It was successfully tested on 18 patients in a phase I clinical trial. All material had been degraded by 4 weeks and the only adverse effect was one stent that migrated into the bladder.

Because of the success of the phase I trial, a phase II trial on 88 patients was performed. The stents were eliminated from the ureter at a median of 8 days and from the body at a median of 15 days. For the majority of patients (78.2%) the stent provided effective stenting of the ureter for 48 hours. Unfortunately, after 3 months stent fragments remained in 3 patients and surgical intervention was required. Due to concern about the fragments, the TUDS never made it to market. [66]

1.3.3.4.4 Uriprene Ureteral Stent by Poly-Med, Inc.

The most recent development in biodegradable technology is a substance called Uriprene^{TM}. Uriprene is a biodegradable polymer composed of L-lactide, glycolide, and copolyester components. The material was tested in a porcine model in 2008 and was found to degrade in 7-10 weeks. Though the stent provided excellent drainage, it lacked axial rigidity making it difficult to advance up the ureter.

The Uriprene stent was improved to degrade faster and provide better axial rigidity. In 2009, the stent was again tested in a porcine model. The degradation time was decreased so that 80% of the stents degraded within 2-3 weeks and 100% of stents were eliminated by week 4. The stent was also very biocompatible in histology and provided adequate drainage. The Uriprene stent currently awaits clinical trials. [67]

2. RATIONALE

Approximately 92,000 ureteral stents are implanted every year in US for the treatment of kidney stones, kidney transplants, and urinary incontinence. [68] Although many new materials have been studied for use in ureteral stents, the majority are still made of polyurethane and silicone. While incremental improvements have been made to the design of stents to make implantation easier and reduce encrustation, the basic ureteral stent design has not changed since 1978 when the double J stent debuted. [34], [67] The two main issues continuously facing ureteral stents are encrustation and the need for a removal surgery. Encrustation occurs on all stents at varying degrees and is especially problematic in longer-term use stents. [27], [52] Removal surgery is a large cost additive ($1,131.27 in hospital fees and $149.36 in service fees. [69]) and also requires patient compliance. Occasionally, patients do not return for the removal surgery and the stent that remains in the body for longer than intended can cause renal failure and even death. [70]–[72] A biodegradable stent could solve both these problems as it has been shown that biodegradable materials reduce encrustation and can safely be removed from the body. [73], [74] In addition, a biodegradable stent could reduce the cost of stenting procedure by as much as 37%.

The goal of this master's thesis project is to develop a biodegradable ureteral stent that is equivalent in effectiveness to stents on the market. The main design / performance criteria included: 1) variable length/diameter; 2) easily implantable using existing techniques; 3) provide adequate flow of urine; 4) biocompatible and reduced encrustation; 5) flexible for patient comfort; and 6) degrade in a controlled manner within

6 weeks to encompass most uses.

Following preliminary screening of various biodegradable polymers, polydioxanone (PDO) was selected as a material of choice to fabricate our biodegradable ureteral stent. PDO was chosen because it was easily processed to gain the desired mechanical properties. Additionally, PDO has exhibited lower inflammation rates when compared to sutures made of Polylactic Acid and Polyglycolic Acid. [75], [76] PDO is most commonly used in sutures (PDS, Ethicon), though it has been studied for use in vascular stents, tracheal stents, and other applications. [77], [78] It is a monofilament homopolymer with consistent morphology and high purity.[79], [80] In the present study, commercially available PDO sutures were obtained and fabricated into a tubular structure to meet the functional requirements of ureteral stents. The project was divided into the following specific aims.

Aim 1: Establish a reproducible process to alter the characteristics of polydioxanone for use as a stent.

Aim 2: Characterize the stent by quantifying its degradation time, flow rate, flexibility, and radial strength and verify that these parameters are adequate for physiological conditions.

Aim 3: Compare the chemical and physical characteristics of processed and unprocessed

PDO to determine the mechanism that changes the material properties of the polymer

3. MATERIALS AND METHODS

3.1 Fabrication of Novel Stent

The spiral-shape stent was created by tightly winding a commercially available PDO suture (PDS, size 3-0 (0.2 mm diameter) Ethicon) around a brass rod (diameter = 3.15 mm, Ace Hardware) by hand. Approximately 1m of suture is required to make a 6cm sample segment. When necessary, a custom rod extension with curls at either end was used to create J-shape anchors modeled after stents currently on the market (Figure 3-2). The ends of the suture were secured onto the rod using stainless steel clips before annealing in an oven (Fisher Scientific) at 100 °C for 24 hours. The stents were then quenched in a deep freezer (Isotemp Base) at -80 °C for 30 minutes. Following removal from the rod, the stents were trimmed of the excess suture and placed in a desiccator immediately to prevent degradation from moisture. All tests were performed within one week of stent creation to prevent any partial degradation of the material. Test specimens that have been annealed and then quenched are referred to as "processed" and all untreated PDO suture is referred to as "unprocessed" in the balance of this document.

Figure 3-1 Detail of Coil Design Demonstrating Tube Flexibility
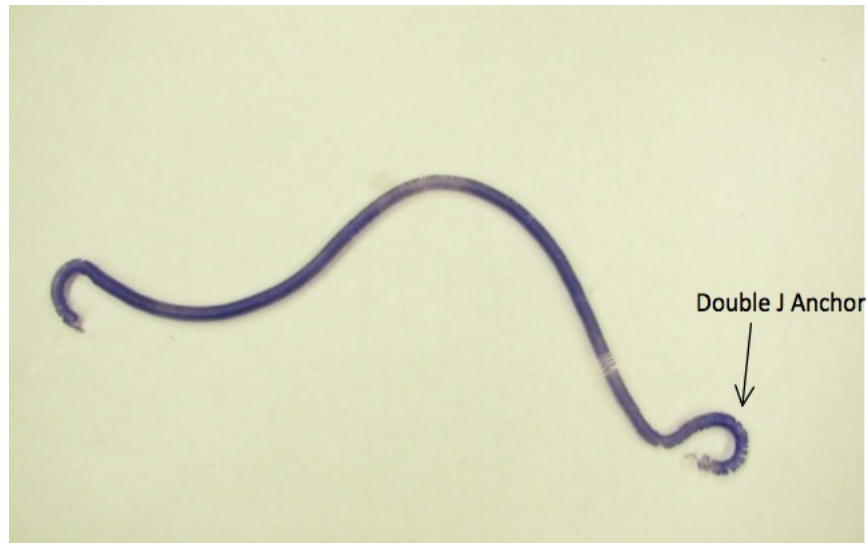
Figure 3-2 Initial Design with Double J anchor

3.2 Designing of Stent Sheath for Novel Anchoring Method

Initial attempts to fabricate a biodegradable ureteral stent were modeled current stents on the market and utilized a standard double J anchor (Figure 3-2). However, implantation using the standard guide wire and push catheter method was very difficult due to the spiral structure creating a high surface roughness. Additionally, initial experiments (in accordance with ASTM standard F1828) found that the anchor strength with the J-anchor design (Figure 3-2) was very low, (<0.03N).

To improve on these limitations, a novel stent implantation and anchoring method, was designed. Specifically, the new anchoring method relied on radial expansion of the stent (I.D 3.15mm and O.D. 3.55mm) during implantation upon release from a silicone sheath (C Flex L/SO.D. 7mm and I.D. 3.1mm). To place the stent inside the sheath, one end of the stent coil was glued to a steel wire and the free end was twisted

until the diameter was less than the inner diameter of the sheath. The stent was fully placed within the sheath by feeding the wire through and the glued end was snipped to allow the stent to uncoil in the sheath (Figure 3-3).
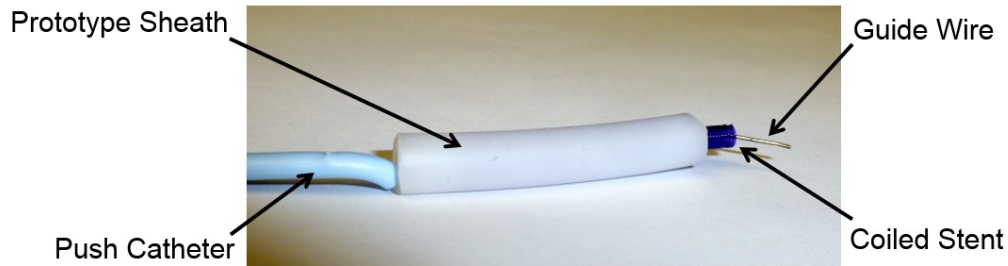
Figure 3-3 Sheath and Stent Implantation Scheme

3.3 Characterization of the Novel Degradable Stent

3.3.1 Degradation of PDO

The mass loss due to degradation was determined by measuring the stent weight change after subjecting the stent to near physiological conditions using a custom-designed ureteral flow simulator. The ureteral flow simulator was kept in a climate controlled room at 37°C to imitate human body temperature. Deionized water circulated through the simulator at 4 mL/min to match the standard flow rate of a ureter. The water resevoir was changed each week to prevent accumulation of degradation byproducts.

The flow circuit (Figure 3-4) consisted of silicone tubing, a peristaltic pump (Fisher Scientific Mini-pump), a 1 L water reservoir, and clear polyethylene tubes. After recording the initial weight, stent samples (6cm long, O.D. 4.15 cm) were placed in

polyurethane tubes (inner diameter of 1.905 cm) to mimic implantation in a ureter. Each week the water in the reservoir was changed to limit the build up of solute concentrations. The stent samples were then removed from the flow circuit and dried in a desiccator under vacuum for 24 hours before weighing to determine mass loss.
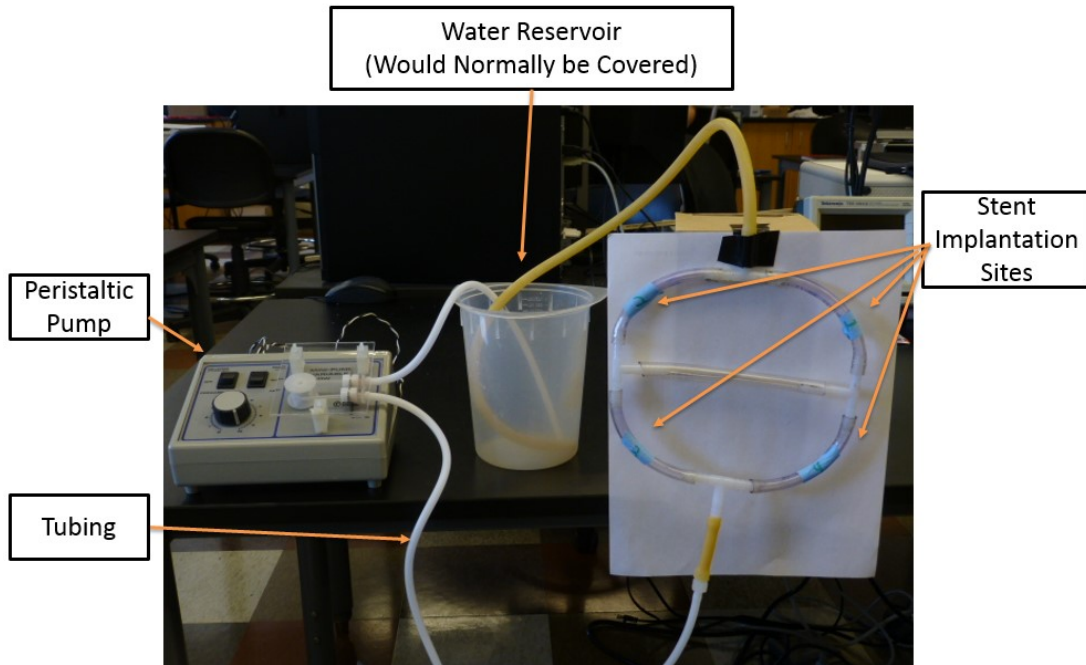
Figure 3-4 Flow Degradation Experimental Setup

3.4 Characterization of Processed PDO

3.4.1 Thermogravimetric Analysis

Thermogravimetric Analysis (TGA) was used to determine the effect of the annealing process on change in mass of the stent. Briefly, after purging with nitrogen, a 4.22 mg sample was subjected to temperature increases at a rate of 20 °C per minute

starting at at 23 °C (room temperature) until the sample reached 600 °C using TA

Instruments Model 2950.

3.4.2 Differential Scanning Calorimetry

First heat, Differential Scanning Calorimetry (DSC - TA Instruments DSC model

2920) was used to determine the effects of the annealing process on the melting point and

crystal structure of PDO.   Small (roughly 5mg) samples of both unprocessed and

processed sutures were subjected to an increasing temperature sweep from -75 °C to 150

°C at a heat rate of 20 °C per minute.

3.4.3 Flexure Testing

Flexural rigidity of unprocessed and processed PDO suture samples was

quantified using a cantilever deflection test adapted from ASTM D747-10. Straight

samples (6 cm in length) were clamped on one end so that 5 cm of sample extended

horizontally and a known weight of 1.025g was hung on the free end. The angle of

deflection in radians was measured and the stiffness was calculated using the following

equation.

$$\theta = \frac{FL^2}{2EJ}. \quad \text{(Eq.\# 1)},$$

where F is the force exerted due to gravity, L is the length of the sample, E is the

modulus of elasticity, J is the polar second moment of area.

For a rod with circular cross sectional area such as the suture, J can be given as

$$J = \frac{\pi}{2} r^4 \quad \text{(Eq.\# 2)},$$

where r the radius of the circular corss section. For this test, r was measured as 0.305 mm.

3.4.4 Fourier Transform Infrared Spectroscopy

To determine chemical composition, Fourier Transform Infrared Spectroscopy (FTIR) was performed on uprocessed and processed PDO suture samples. A small shaving (≈1 g) of each material was made with a stainless steel razor blade to create a flat surface for adequate contact with the focusing crystal. The samples were tested using a Thermo-Nicolet Magna 550 FTIR Spectrometer with a Thermo-SpectraTrech Endurance Foundation Series Diamond ATR. The resulting absorbance curves were then analyzed using standard absorbance tables [4] to verify the chemical purity of the initial PDO samples and to verify that there was no chemical change during processing.

3.4.5 Wide Angle X-Ray Scattering

Wide angle X-ray scattering with Cu Kα1 radiation at λ = 1.54060 Å was performed on both unprocessed and processed PDO suture samples using a Rigaku Ultima IV X-ray diffractometer to compare the degree of crystallinity. To allow consistent absorption of X-rays, suture was cut into pieces of varying length and arranged in parallel on the circular aluminum sample pan to create a solid, consistent sample layer. Likewise, processed PDO samples were created in a straight orientation instead of the normal "coiled" orientation and arranged into a solid layer. After initial scanning at an

angle from 5°-60° for 3 hours, the peaks of interest were identified and a second scan was run from 5°-35° for 3 hours.

3.4.6 Inherent Viscosity

To determine the molecular weights of the processed and unprocessed PDO suture samples, the inherent viscosities were determined. Processed and unprocessed PDO （0.25m g each） was dissolved in 15 mL of hexafluoroisoproponal (Oakwood Chemicals) with agitation at room temperature for 24 hours. The PDO solutions in hexafluoroisoproponal were then decanted into size I Ubbelholde capillary viscometers (Cannon Instruments) and allowed to equilibrate in a water bath at 25 °C for 10 minutes. The inherent viscosity was measured by viscometric analysis according to ISO 1628-1:2009.

Briefly, before testing the PDO samples, the viscometer was rinsed with HFIP to remove any potential contamination. Ten mL of HFIP was then decanted into the viscometer and nitrogen was used to force the HFIP up the viscometer capillary. A stopwatch was used to measure the time it took for the HFIP to flow through the viscometer capillary while recording the time it took. This process was repeated 5 times and the average time was calculated to establish a "Sample Efflux Time". After the HFIP was removed and the viscometer was dried by flushing with nitrogen, the PDO solution was tested in the same manner to determine a "Solvent Efflux Time". Using the Sample Efflux Time and the Solvent Efflux Time, the Relative Viscosity (η_{Rel}, Eq. #3) and the inherent viscosity were calculated (Eq. # 4).

$$\eta_{Rel} = \text{Sample Efflux Time} \div \text{Solvent Efflux Time (Eq.\# 3),}$$

$$\eta_{Inh} = \ln(\eta_{Rel}) \div \text{Solution concentration (in g/dl) (Eq. \# 4.)}$$

3.5 Validation of Implantation Method

Fresh porcine ureters were harvested on site at Snow Creek Meat Processing (Seneca, SC) and stored in 500mL of saline solution on ice and transported to the laboratory for use on the same day. After a 6 cm long stent was packaged in the silicone sheath (as described in 3.2) the entire structure was placed on the guide wire. The guide wire was threaded through a 6 cm long ureter segment and the sheath was slowly pushed into the ureter using a push catheter. Simultaneously, the sheath was retracted to force the stent out of the sheath. Upon leaving the sheath, the stent uncoiled to its original diameter and anchored itself in the ureter (Figure 3-5). Upon implantation the stent was used for anchor strength and flow testing.

Figure 3-5 Two Implanted Stents with Unimplanted Stent for Comparison

3.5.1 Anchor Strength Testing

Initial anchor strength testing was attempted via an adaptation of ASTM F1828-97 using MTS Synergie 100 with 10N load cell. The stent was implanted into a ureter segment as described in section 3.5 The specimen was submersed in a reservoir with 0.5 L of DI water at 37 °C during the test. The top of the stent was grasped by the top grip and the ureteral segment was attached to the bottom grip. The stent was pulled out of the ureter at rate of 20mm/min. The maximum force detected was given to be the anchor strength. However, during the test, it was observed that the stent uncoiled and elongated. Additionally, a very large extension was required for the stent to pull out of the ureter and the results varied greatly.

To provide a more repeatable and physiologically relevent test, the method of attaching the stent to the grip was modified. All experimental conditions were the same except a 12-gauge steel wire was threaded through the stent and glued with epoxy to the bottom end of the stent. (Figure 3-6) The "push wire" was then attached to the top grip of the MTS machine and the ureter segment attached to the bottom grip. The wire was pulled at a rate on 20 mm/min, applying force to the bottom of the stent, until the stent became dislodged from the ureter.
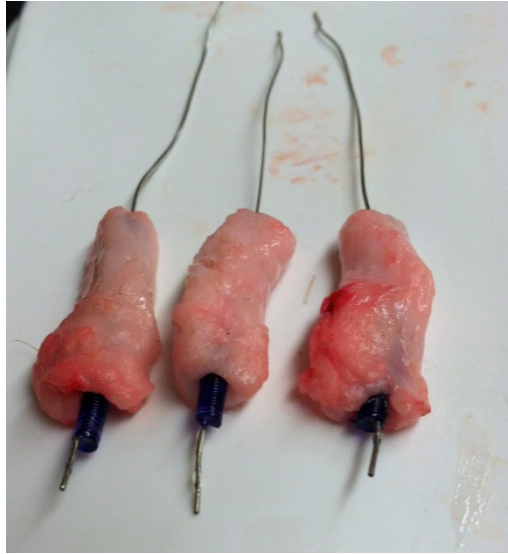
Figure 3-6 Stent Anchor Strength Experimental Setup

3.5.2 Flow Rate in a Stented Ureter

The maximum flow rate of water through a stented ureter was measured to verify that the stent would not impede drainage of the kidney. To test this, a 3.9 cm long stent segment was placed in a 4 cm long ureter (as described in section 3.6) and a fixed volume (50 mL) of DI water was flowed through the ureter while the time was recorded. This process was repeated 10 times to obtain statistically meaningful data.

3.6 Radial Strength Testing

To determine the radial strength of the stent, a novel testing device was designed, assembled, and calibrated. A 6 cm long flexible polyethylene sleeve with a closed end, was attached to a 500 mL rigid polyethylene canister such that the inside of the sleeve was exposed to atmospheric conditions while the outside of the sleeve was exposed only

to the interior of the chamber. A 6cm stent segment was placed in the flexible sleeve. A 12V air pump (Airpo D028B) was connected to pressurize the chamber and to apply a radial force uniformly across the stent encased in the sleeve (Figure 3-7).

Pressure Chamber

Figure 3-7 Diagram of Radial Strength Testing Device
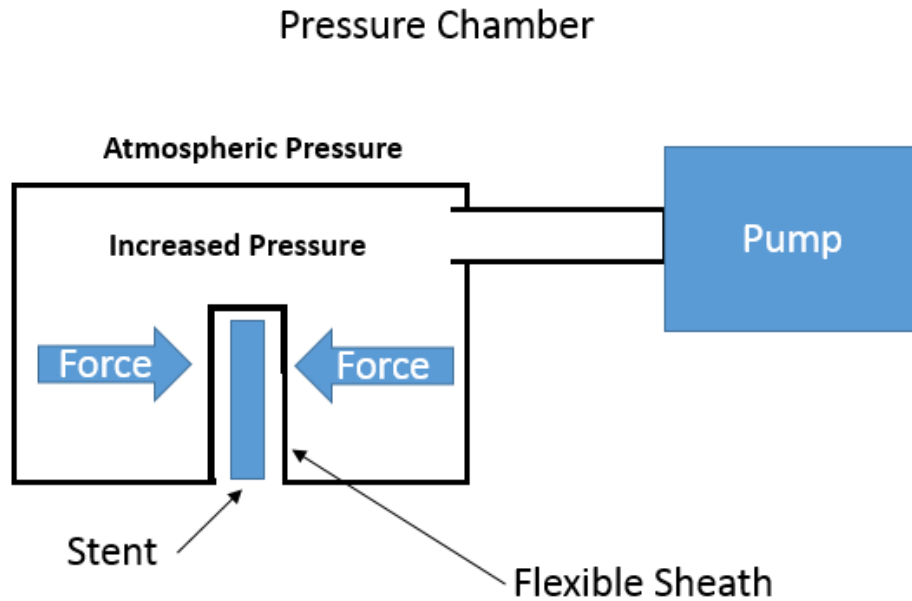
To monitor the pressure in the chamber, an Arduino Blue Tooth Microcontroller (Smart Projects, Italy) with a custom program (appendices) and an attached Adafruit BMP085 pressure sensor (Sparkfun, Boulder, CO) were used (Figure 3-8). During testing, the pressure was recorded in realtime via a bluetooth connection to a computer (Apple, Macbook pro) and deformation of the stent was monitored visually. The pressure data were converted to radial force by multiplying the pressure by the area of the sheath. The maximum force exerted on the stent was determined and reported as the radial strength of the stent.
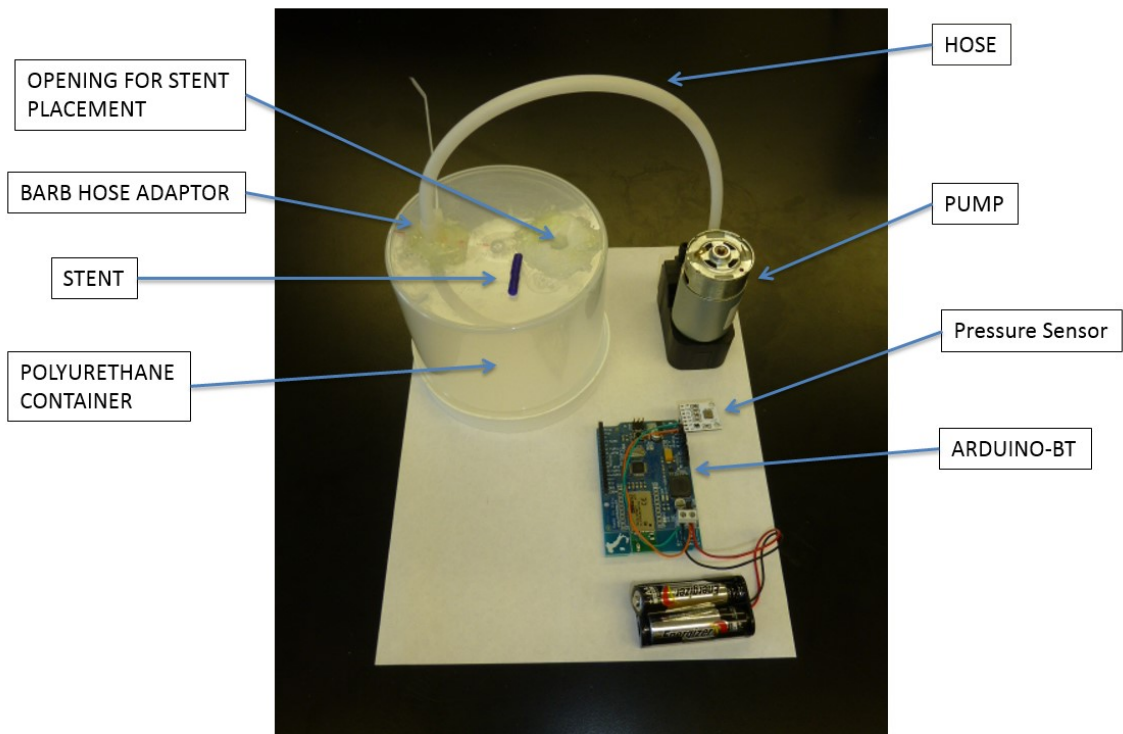
Figure 3-8 Completed Radial Strength Testing Device

3.7 Statistical Analysis

All results are expressed as the mean ± standard deviation of the mean . All statistical analysis was performed using single factor analysis of variance (ANOVA). Differences between the means were determined using least-significant difference with a significance level of α=0.05. Error bars shown are the standard deviation of the mean.

4. RESULTS

4.1 Characterization of Stent Degradation

4.1.1 Mass Loss of Stent due to Hydrolytic Degradation

The mass of all the stents remained nearly constant ($0.14g \pm 0.01g$ $p = 0.14$) during the

three week flow circuit degradation test. (Figure 4-1) After four weeks, however, the

stent had crumbled and small stent fragments (<1g) had been flushed into the water

reservoir. The degradation test was then terminated at that time point.
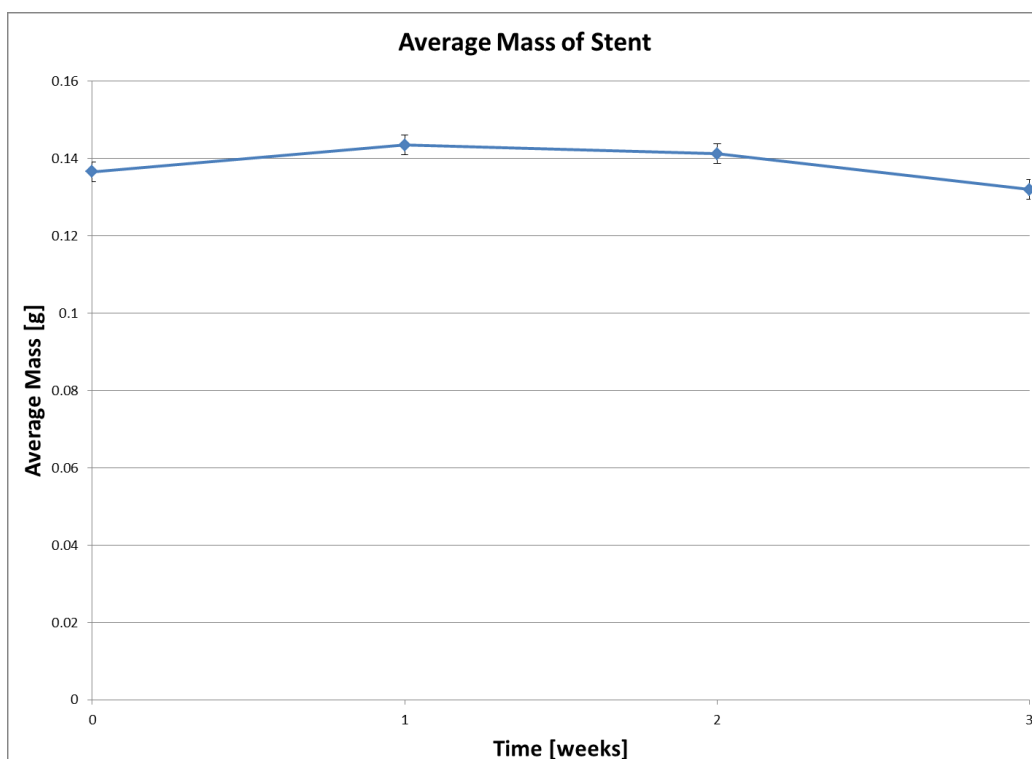
Figure 4-1 Average Mass Loss of Stent Over Time

4.2 Physical Characterization of Stent

4.2.1 Thermogravimetric Analysis of Processed Stent and Unprocessed Suture

To determine the thermal stability of the processed and unprocessed PDO suture, TGA was performed. (Figure 4-2) The results of TGA indicated that both samples started losing mass at 200 °C and reached 0% mass at approximately 350 °C. However, the processed stent started losing mass at a faster rate than the unprocessed suture. This indicates that stent is degraded and has lower molecular weight polymer chains which are more easily volatilized. Holding the stent at 100 °C kept the stent showed no change in mass.
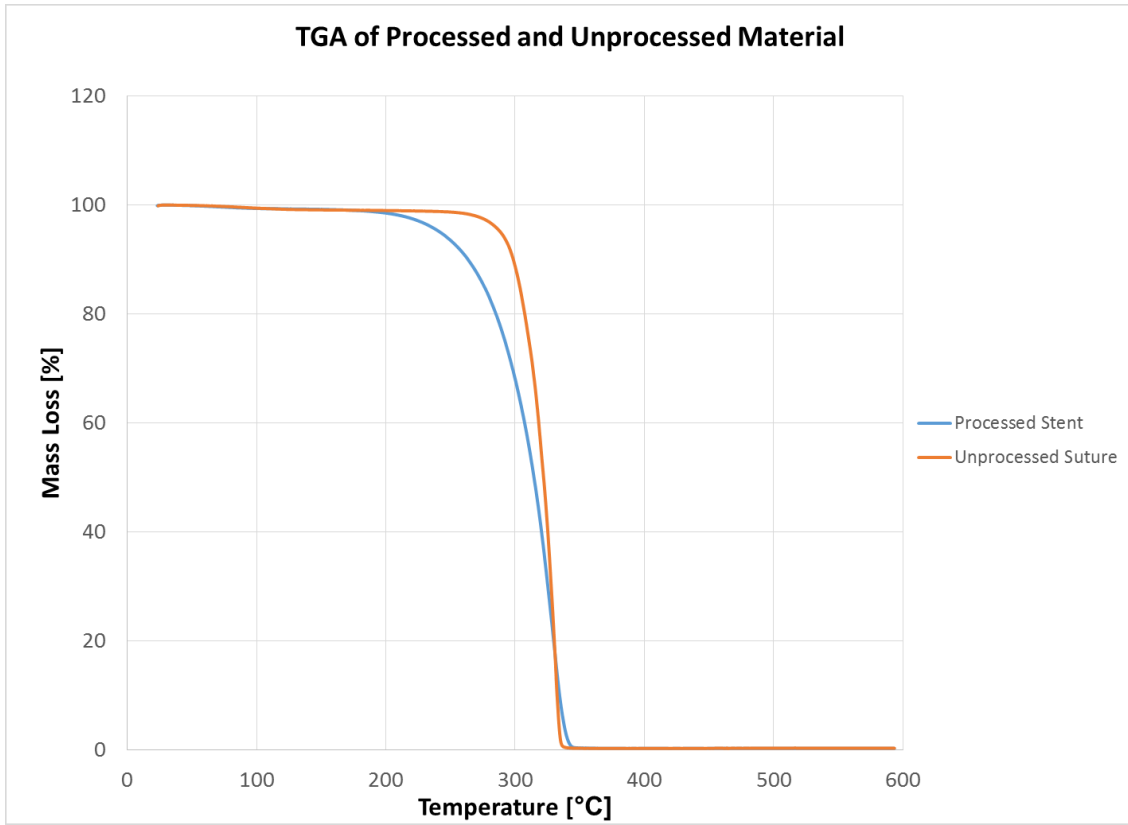
Figure 4-2 Plot of Thermogravimetric Analysis of Annealing Process Over 6 Hour Period

4.2.2 Differential Scanning Calorimetry

Differential scanning calorimetry (DSC) was used to determine the potential change in crystallinity of the polymers due to annealing by calculating the enthalpy of melting. First, the DSC established that each sample was a single material and phase (semi-crystalline) as shown by the single peak (Figure 4-3). The melting temperature (Figure 4-4) was determined as the temperature at which maximum heat flow was present represented as the lowest point on the curve. The enthalpy of melting for each material (Figure 4-5) was determined by integrating the area of each melting peak in DSC plots.
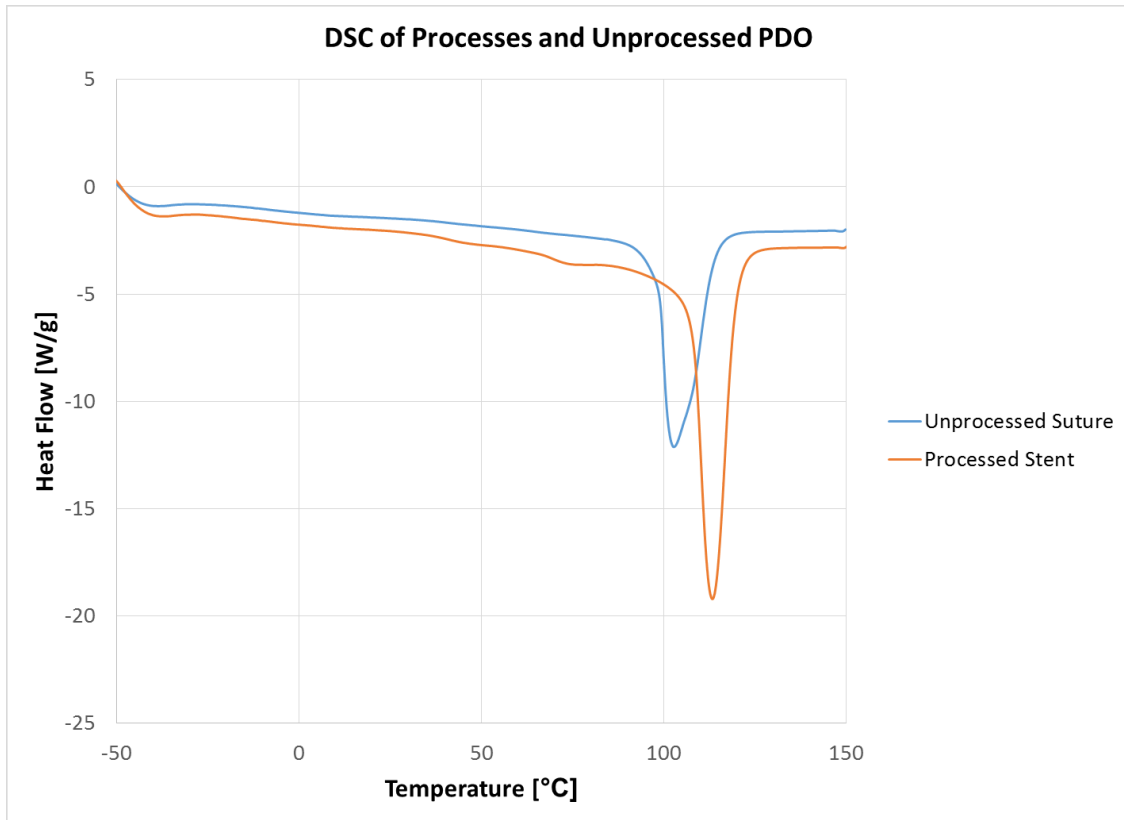
Figure 4-3 Representative Differential Scanning Calorimetry Curve of Processed Stent and Unprocessed Suture
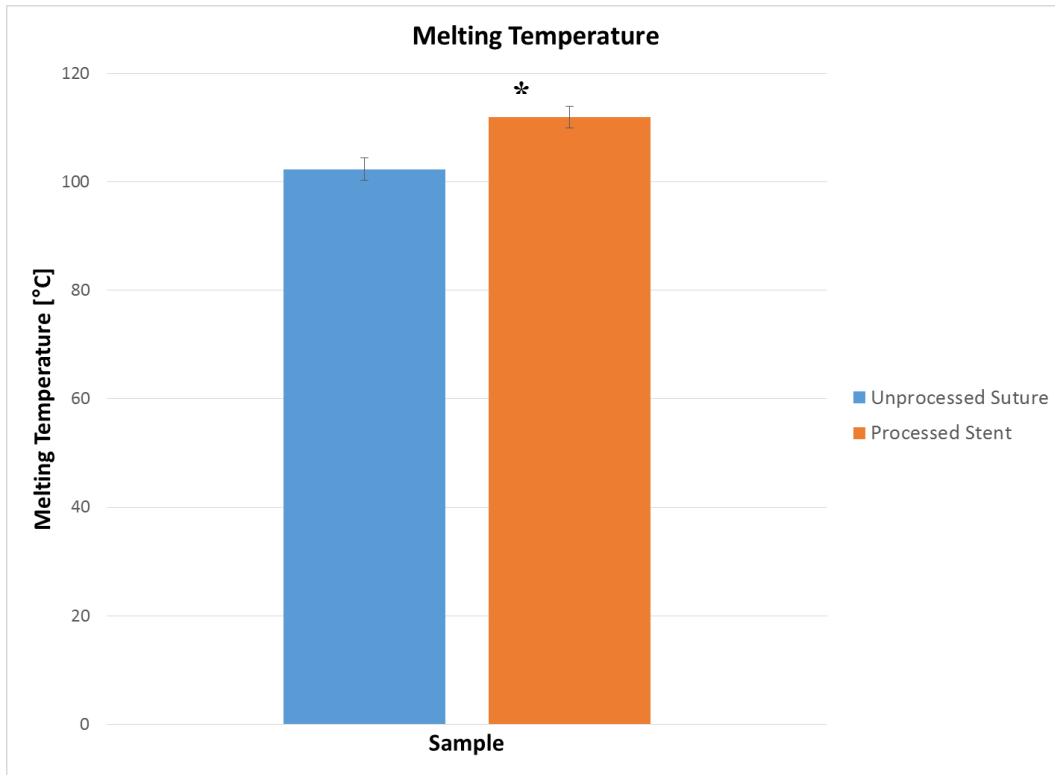
Figure 4-4 Melting Temperature of Processed and Unprocessed Suture (Data are mean ± standard deviation *p= 0.001 analyzed by ANOVA, n=4)

The processed stent exhibited a significantly (p=0.001) greater average melting temperature (111.89±2.01 °C) compared to that of unprocessed suture (102.32±0.50 °C) (Figure 4-4). The enthalpy of melting of the processed stent (105.19±16.10 J/g) appeared greater than the unprocessed suture (92.68±9.30 J/g) (Figure 4-5). However, the variance of the enthalpy of melting values was high enough such that they cannot be considered statistically different. The increase in melting point indicates that the material is gaining crystallinity post processing.
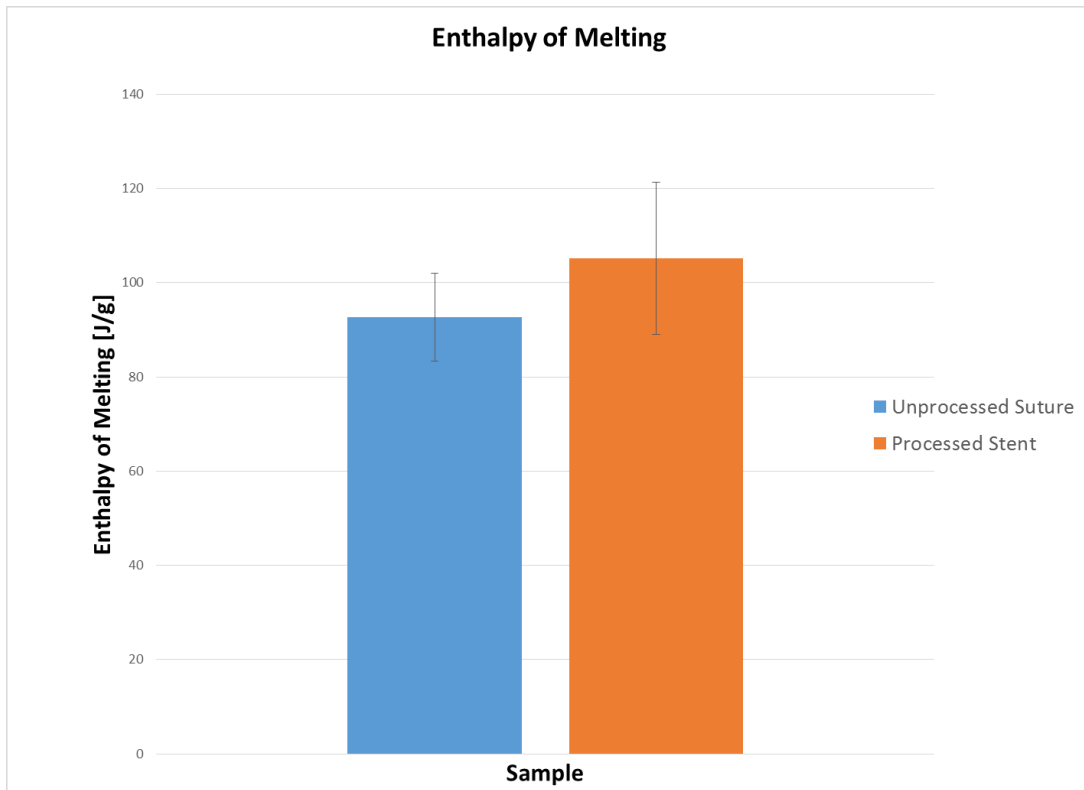
Figure 4-5 Enthalpy of Melting of Processed and Unprocessed Suture (Data are mean ± standard deviation p= 0.308, analyzed by ANOVA n=4)

4.2.3 Fourier Transform Infrared Spectroscopy

Fourier transform infrared spectroscopy (FTIR) was used to determine the potential chemical change of PDO underwent any chemical change during the 24 hour annealing process.
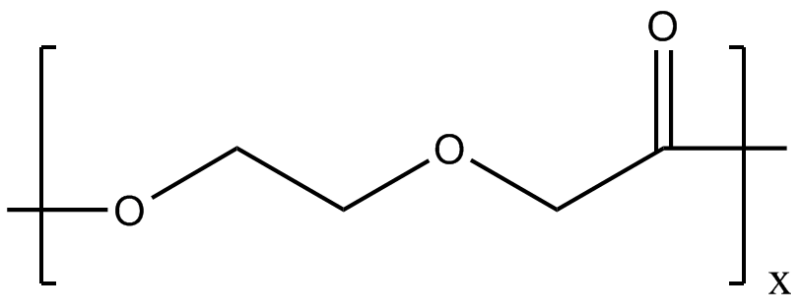
Figure 4-6 Chemical Structure of Polydioxanone

The results of FT-IR revealed the presence of the single ketone peak at 1700 cm^{-1} for both unprocessed and processed suture samples which matches the expected structure (Figure 4-7). The multiple peaks in the 1000-1200 region verify the presence of multiple ether groups (Figure 4-7) and their identical locations indicated that chemical structures were not influenced by the heat processing.
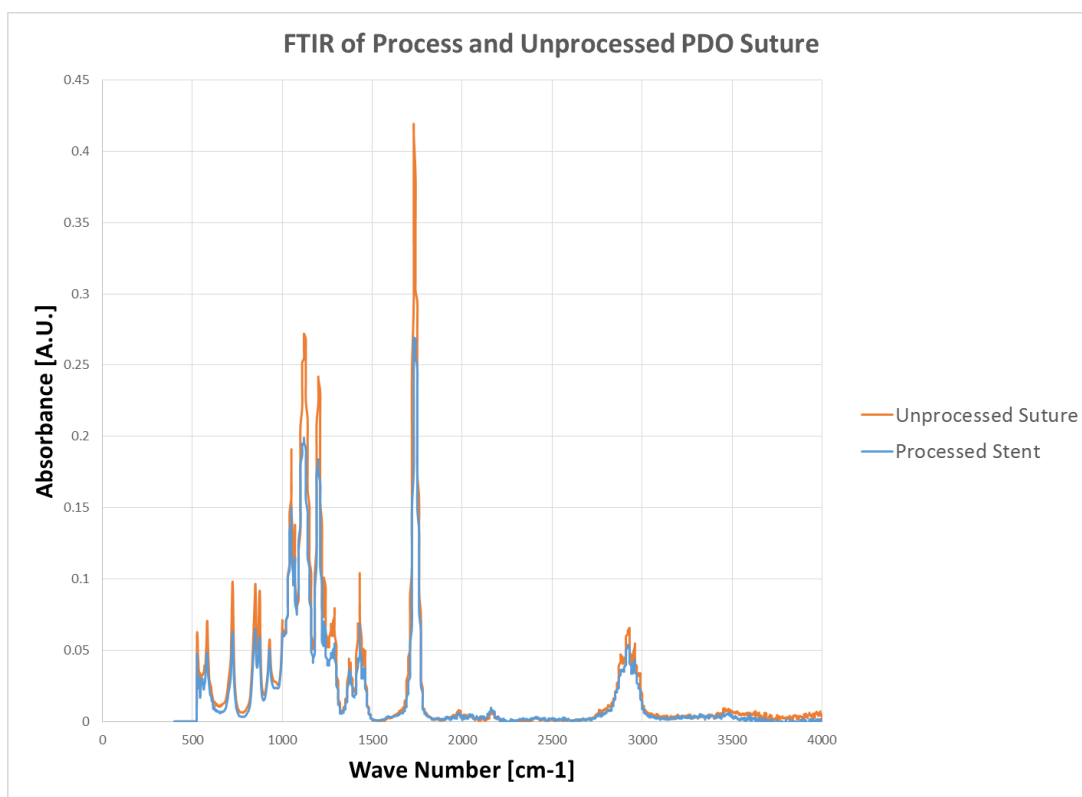
Figure 4-7 Representative FTIR Curve of Processed Stent and Unprocessed Suture

FT-IR results for processed stent and unprocessed suture showed similar peaks after 6 months of storage indicating that no chemical change in polymer took place over this time period. The lack of additional peaks shows that there was no contamination with other materials during storage.

4.2.4 Wide Angle X-Ray Scattering

Wide Angle X-Ray Scattering was used to determine the relative amount of crystallinity in unprocessed and processed sutures. The initial "scan" between 5 and 60 degrees revealed peaks at roughly 23 degrees, 38 degrees, and 45 degrees. (Figure 4-8)

The peaks at 38 degrees and 45 degrees were known historically to be a result of diffraction from the aluminum sample pan and were not studied. The peak at 23 degrees was deemed the intensity peak of PDO.
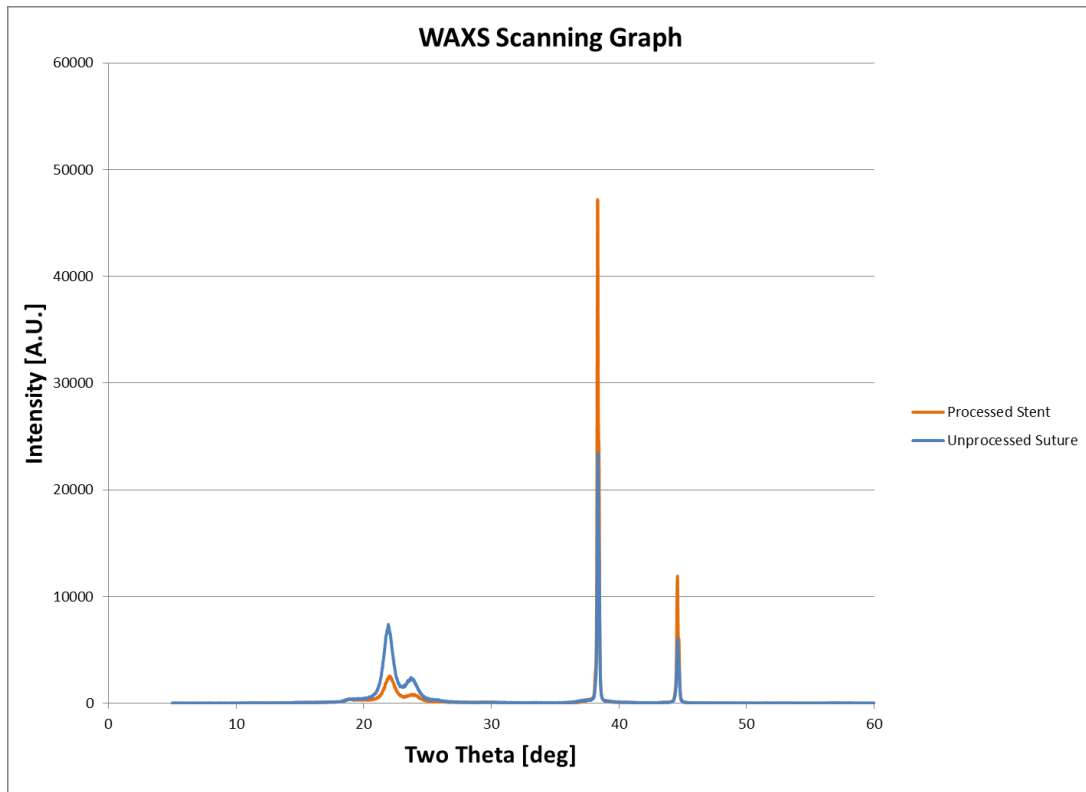
Figure 4-8 Initial "Scanning" for Peaks Using WAXS

The peak of interest was scanned with a greater intensity (Figure 4-9). While unprocessed suture exhibited a major peak of 4512 at 21.62 deg and a lesser peak at 21.88 deg, the processed stent exhibited a peak of 4953 at 21.88 deg and 23.60 deg. (Figure 4-10), this corresponds to 9% increase in intensity from the suture to the stent.
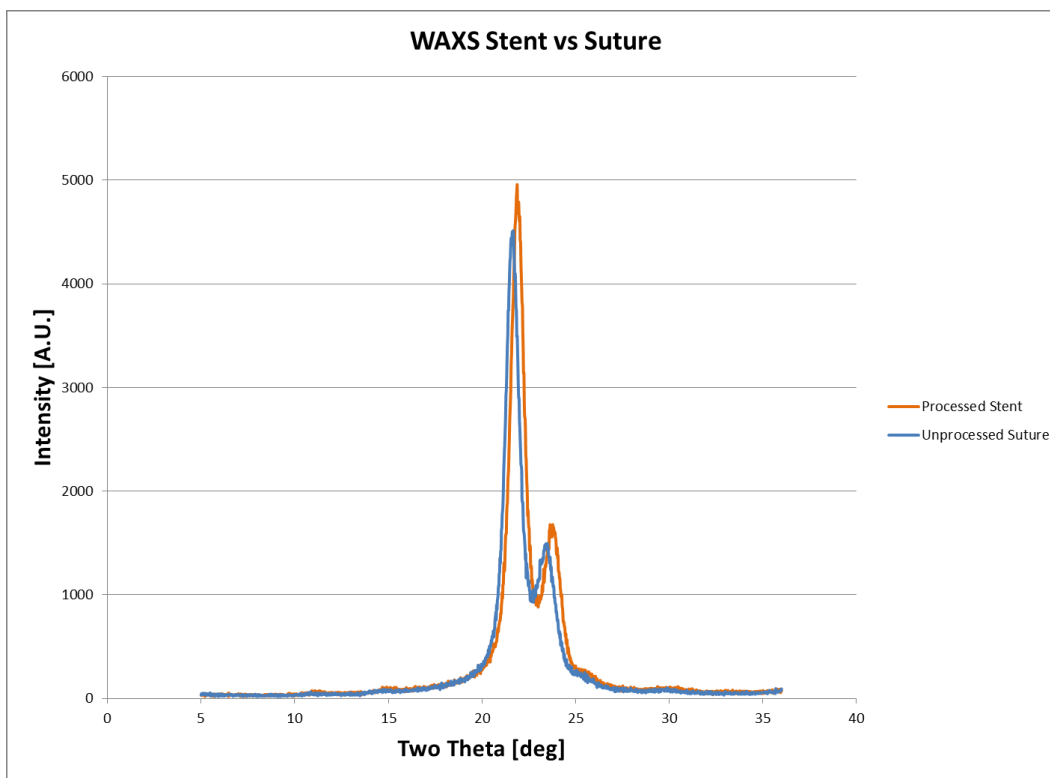
Figure 4-9 Representative Wide Angle X-ray Scattering Curve of Processed and Unprocessed Material

4.2.5 Viscometry

To determine the relative change in molecular weight of PDO sutures due to heating at 100 °C for 24 hours to fabricate stents, viscosity measurements of the unprocessed and processed polymers were compared and the results are shown in Figure 4-10. The average kinematic viscosity of the unprocessed suture, 1.58±0.07 dL/g, was significantly higher (p=0.002) compared to that for processed stent, 1.38±0.07 dL/g. This indicates that the molecular weight of the suture is higher than that of the stent.
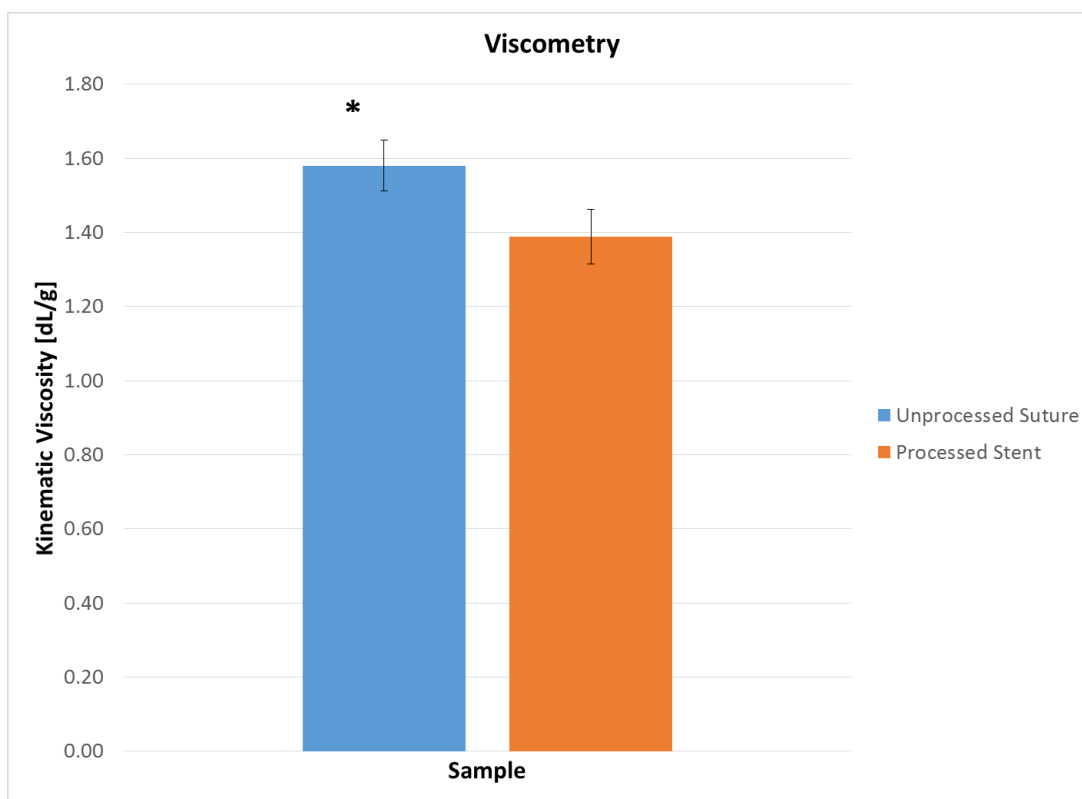
Figure 4-10 Comparison of Kinematic Viscosity of Processed and Unprocessed Material (Data are mean ± standard deviation p=0.002, analyzed by ANOVA n=5)

4.3 Mechanical Characteristics

4.3.1 Flexural Stiffness

Flexural stiffness of processed and unprocessed suture was quantified by deflection testing 6, 12, and 24 hours after processing of the material. The flexural stiffness of the original suture material determined from the deflection test was 47.9±5.8 MPa with no processing time, 50.3±4.0 MPa after 6 hours, 58.74±4.57 MPa after 12 hours and 65.5±3.8 MPa after 24 hours of processing. This represents an increase in the stiffness by 27%, during the standard stent processing time.
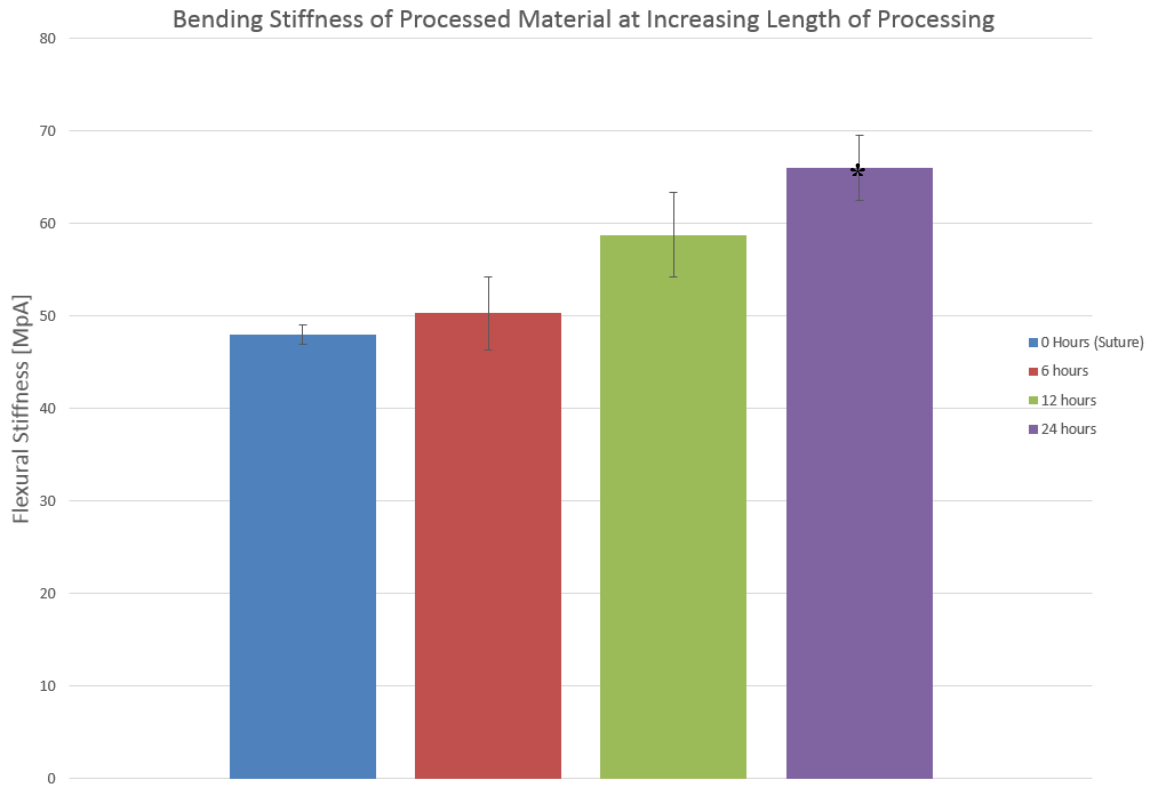
Figure 4-11 Flexural Stiffness of PDO at Increasing Processing Times (Data are mean ± standard deviation p=0.011, analyzed by ANOVA n=5)

4.3.2 Flow Rate of Stent

The average flow rate of deionized water through a 3.9 cm stent segment placed in a porcine ureter was 1.74±0.55 mL/s under the test conditions of the present study (Table 4-1).

	Trial 1 [mL/s]	Trial 2 [mL/s]	Trial 3 [mL/s]	Average (+/- SD) [mL/s]
Run 1	1.57	1.66	1.00	1.41±0.36
Run 2	2.12	2.62	2.43	2.39±0.25
Run 3	2.26	1.24	1.39	1.63±0.55
Average (+/- SD)	1.98±0.29	1.84±0.58	1.61±0.60	1.74±0.55

Table 4-1 Flow Rate through Explanted Porcine Ureter with 3.9 cm Long Stent Segment

4.3.3 Radial Strength

In testing with the custom device that applied increasing radial compression, the stent withstood a pressure of 30 KPa without breaking or buckling. (Figure 4-12).
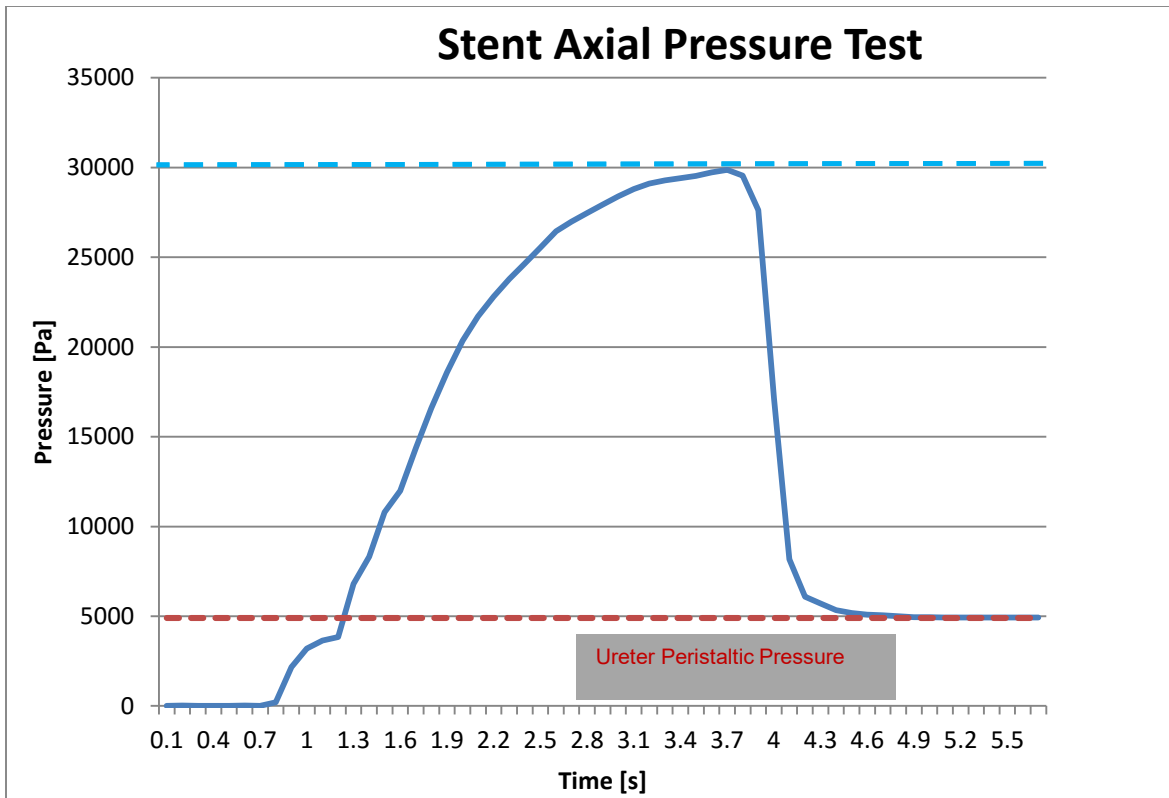
Figure 4-12 Radial Pressure Over Time

4.3.4 Anchor Strength

Initial testing where the stent was "pulled" from the top was found to be inconsistent with an average force of 0.06±0.06 N for a 3.0 cm segment. (n=3). A representative curve is shown in Figure 4-13. The average anchor strength of a stent in a porcine ureter using the method where the stent was "pushed" from the bottom was found to be 1.09±0.26 N for a 3.9 cm segment (n=3). (Figure 4-14) This anchor strength would be substantially larger for a full length stent, and estimated at 7.82 N for a standard 28 cm long stent.
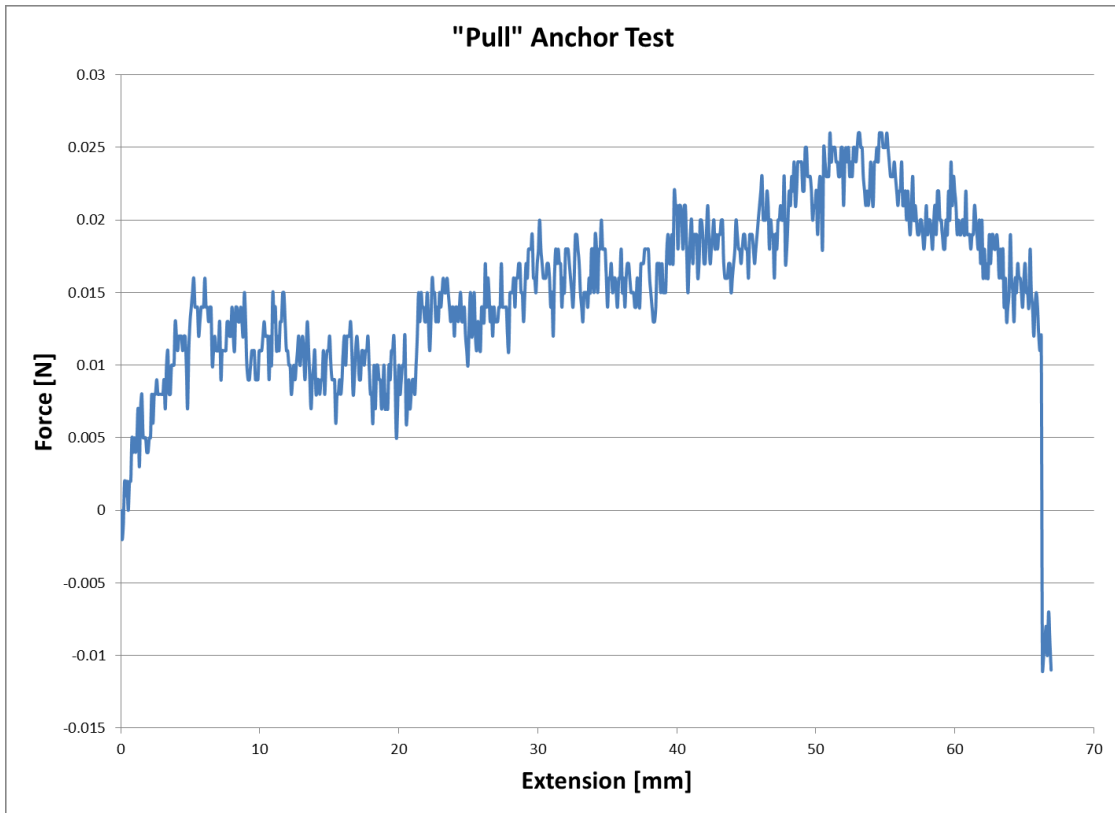
Figure 4-13 Representative Curve of Force vs Extension of an Implanted Ureter with "Pull" Anchor Method
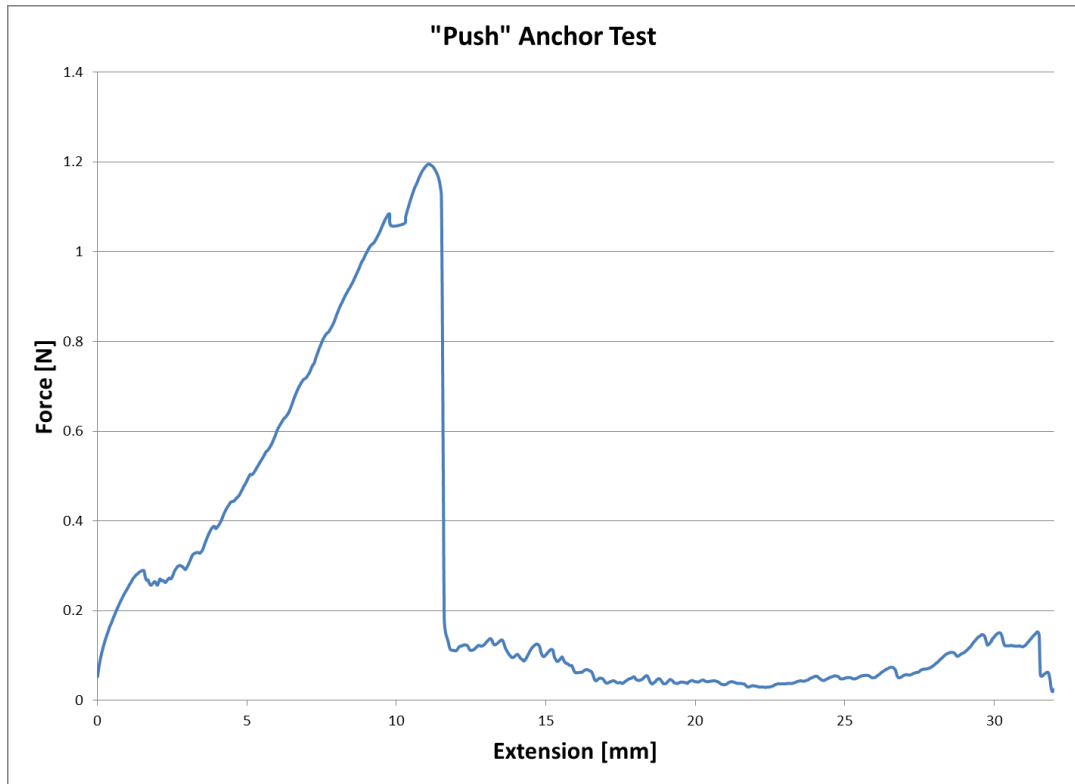
Figure 4-14 Representative Curve of Force vs Extension with "Push" Anchor Method

5. DISCUSSION

Approximately 92,000 ureteral stents are implanted every year in US for the treatment of kidney stones, kidney transplants, and urinary incontinence. [68] Although many new materials have been studied for use in ureteral stents, the majority are still made of standard plastics such as polyurethane and silicone. While incremental improvements have been made to the design of stents to make implantation easier and reduce encrustation, the basic ureteral stent design has not changed since 1978 when the double J stent debuted. [34], [67]

The two main issues continuously facing ureteral stents are encrustation and the need for a removal surgery. Encrustation occurs on all stents at varying degrees and is especially problematic in longer-term use stents. [27], [52] Removal surgery is a large cost and also requires patient compliance. Occasionally, patients do not return for the removal surgery and the stent that remains in the body for longer than intended can cause renal failure and even death. [70]–[72] A biodegradable stent could solve both these problems as it has been shown that biodegradable materials reduce encrustation and can safely be removed from the body. [73], [74]

The goal of this thesis project was to design a stent that solves many of the difficulties presented by the current stents on the market. In pursuit of this goal, a novel stent was fabricated by heat-treating a commercially available PDO surgical suture and shaping it into a coiled tube. To test its performance, the present study characterized the stent's degradation profile, chemical composition, and mechanical properties.

5.1 Design Criteria and Innovative Features

5.1.1 Spiral Structure

Standard biodegradable polymers such as, PDO, PGA, and PLA are too stiff to be used in a solid walled stent. The spiral design was created in an attempt to utilize these polymers to create a structure that is both radially stiff and has sufficient axial flexibility. The stent needs to be radially stiff to hold open a lumen that would otherwise be closed due, for example, to inflammation, structure, pressure from a tumor, or a naturally occurring stricture. The axial flexibility is required for the stent to accommodate the sharp angle from the urethra into the ureter and to improve the patient comfort as movement at the waist, such as sitting causes the ureter to bend.

5.1.2 Polydioxanone as Material Choice

In the present study the polydioxanone (PDO) suture was annealed and then quenched to create a stiff material that holds the coiled structure with the desired flexibility and provides radial strength. The annealing temperature 100 °C was chosen based on the melt point at roughly 110 °C and the quenching at -40 °C greatly controlled the process and polymer's crystallinity. PDO was chosen as the ideal material because its shape setting allows the polymer to maintain the stent in coiled shape. Additionally, PDO was ideal for this application because it has a degradation profile in line with that desired in the ureteral stent application. It has been shown to exhibit a strength loss after about 15 days with full degradation occurring by 80 days. [81] This was confirmed by the degradation data obtained in the present study.

5.1.3 Implantation Method

The standard ureteral stent implantation begins with the urologist guiding a wire into the urethra, though the bladder, and into the ureter. A ureteral stent is placed on the guide wire and is pushed into the ureter with a push catheter. The guide wire and push catheter are then removed allowing the j-shape anchors to curl in both the kidneys and the bladder to keep the stent in place. However, because of the spiral structure of the stent, this implantation method could not be used. Pushing on the end of the stent would cause it to expand and increase its diameter prior to entering the ureter. To this end, a sheath to hold the stent in place during implantation was developed. A stent segment would be twisted to reduce its diameter and packaged inside the sheath. Once implanted in the ureter, the stent could be pushed out of the sheath with a push catheter and recoiling action would ensure anchoring in position. In the present study, a 3.9 mm stent segment was successfully implanted in vitro in a porcine ureter with this method. However, it was discovered that removal of the stent, via the push catheter, from the sheath into the ureter was very difficult by hand. This is because the stent was anchored in the silicone due to its tighter coil. A sheath made of a smoother material would allow the stent to more easily be forced out. While the inclusion of the sheath in the implantation procedure does add some complexity, it does provide some benefits.

5.1.4 Benefits of Novel Anchor Method

The entirety of the coiled stent comes in contact with the ureteral wall as means of preventing stent migration instead of the conventional J-shape anchors on the distal

(kidney) and proximal (bladder) ends. This provides benefits over the standard design. First, a standard double J stent requires the stent to be long enough for the ureter to extend and not contact the anchors. The downside to this is that with the ureter at a shortened position, the stent extends well past the end of the ureter into both the kidney and bladder. Typically, an implanted stent is at its longest in the supine position and compresses and shortens by approximately 2.1 cm (1.8 to 3.9 cm) between standing, bending, and sitting positions. [82] During these periods the stent can press against the top of the kidney or the base of the bladder, which causes severe pain or feelings of urgency. The proposed coiled stent design allows the stent to expand and contract as needed, like a spring, without going into the bladder or into the kidney.

Additionally, the removal of the proximal anchor should allow the stent to sit above the vesicoureteral junction. This should prevent the

Finally, it has been demonstrated that the distal anchor that sits in the kidney is most prone to encrustation. [71] Thus, it is believed that the omission of distal anchor will provide less opportunity for degradation as there will no longer be material present in the more solute concentrated environment of the kidney.

5.2 Mechanical Characterization

5.2.1 Effects of Annealing on Flexural Stiffness of PDO Suture

Flexural stiffness was determined via cantilever bend test adapted from ASTM D747-10 and used as an indicator of the changes in the stent material due to annealing. The material was found to increase in stiffness by 27% (Section 4.3.1, Figure 4-11),

which is believed to be due to the increase in crystallinity. This is because the polymer

chains are more ordered and thus share dispersion forces (also known as Vander Waals)

more than an amorphous material. This increase in dispersion forces causes the chains to

resist movement which equates, on a macro scale, to an increase in stiffness. [83] The

increase in the stent stiffness was a desired feature to withstand ureteral force and to

allow the stent to maintain its shape.

5.2.2 Radial Strength

The ASTM standard test for ureteral stent radial strength requires compression

between two parallel platens and not applicable for our helical stent design because of its

geometry. To reflect physiological loading condition the where the peristaltic contraction

forces of the ureter would be placed from all sides, a new test method was developed.

Our stent withstood pressure up to 30,000 Pa without any buckling or fracture. This is

much higher than the reported maximum peristaltic pressure of 5000 pa from the ureter,

indicating that the stent has adequate radial strength. This would be analogous to the

result of ASTM F 1828-97 Standard Specification for Ureteral Stents. [84], [16]

Ureteral stents currently on the market are typically made of silicone or

polyurethane. These polymers can be molded into a continuous tube and provide enough

radial stiffness to maintain patency. However, because they are composed of a single

polymer, ensuring the stiffness in the radial directions also causes high stiffness of the

stent in the axial direction. While the stents are flexible enough to be implanted, patient

discomfort is frequently reported. [85]   In addition, a soft material is more likely to

accidently kink when bent such as when the implanted stent shifts from patient movement. Thus, it is believed that the combination of stiff, annealed PDO with the spiral design will provide better patient comfort.

5.2.3 Flow Rate

The fluid flow rate through the biodegradable stent was measured using water and a stent segment implanted vertically in a straight porcine ureter. This would correspond with stent implanted while a patient is sitting or standing. The results demonstrated that the average flow rate of urine through the ureter with the implanted stent segment was 1.74±0.55 mL/s (Section 4.3.2, Table 4.1).

The standard flow rate of urine through a ureter varies drastically depending on hydration and patient anatomy but it is typically derived from the standard production rate of urine. In the urinary system, urine is produced in the kidney at a gradual rate where it is stored in the bladder for voiding. Thus, an average value for the flow rate is typically found by averaging the total measured urine output of the body over a given time. This yields a flow rate of 0.008-0.167 mL/s for the average flow rate of urine through the ureter. [7], [86] Because our stent is capable of allowing urine to flow at a rate approximately 10 times that the reported values, it is believed there will be adequate draining post implantation.

5.2.4 Anchor Strength

Our initial attempt to test the anchor strength of an implanted stent was unsuccessful as the stent exhibited a very low anchor strength with high variability 0.06±0.06 N. Additionally, instead of the expected behavior of the stent pulling out of the ureter, the stent elongated to over twice the normal length and slipped out of the ureter slowly. This resulted in an inconsistent force vs deflection curve (Figure 4-13), with each ring slipping out and creating sharp increases and decreases in measured force. Finally, after pulling free from the ureter, the stent sprang back into shape, providing the negative force seen at the end of the curve. This is not believed to accurately represent the mode in which an anchored stent would become dislodged in the body. Stent migration is predominantly toward the bladder and is a primarily due to backpressure from urine and peristaltic forces.[32] This necessitated a change in design of the stent to include a radial expansion anchor method and a sheath for implantation. However, due to the sheath design, the ASTM F 1828-97 anchor strength test was not applicable as there was not a curl to pull against. Thus, a novel test methodology was implemented.

It was desired to update the anchor strength test to better simulate this physiologic condition by applying a "push" similar to peristaltic forces instead of the "pull" of the standard test. This was accomplished by threading a wire through the stent and fastening it to the bottom of the stent, so that the top grip of the MTS machine can apply force to the bottom of the implanted ureter. In this test, explanted porcine ureters were used to provide a surface for the stent to anchor to. The force vs deflection curve (Figure 4-14) exhibited an initial elastic region of the graph which is attributed to the ureter itself

elongating and resisting the applied force. After roughly 1 cm of extension, a sharp

decrease in detected force is observed, this is believed to be the point at which the stent

moves within the ureter. There then follows a region of, low uneven force which

corresponds with the individual rings of the stent slipping from the ureter. The anchor

strength of a stent in a porcine ureter using this was on average 1.09±0.26N for a 3.9 cm

segment, which may be extrapolated to 7.82 N for a standard 28 cm full-length stent.

This is substantially higher compared to the strongest reported anchor strength values of

0.73 N and 0.62 N for the 6 french Cook Black Silicone and the Cook C- Flex stents

respectively. [87] Thus, it is believed that the proposed stent design will have adequate

anchor strength to operate in a clinical setting.

5.3 Characterization of Stent Degradation

To determine the rate of mass loss, an ex-vivo study was performed in a manner

similar to physiological conditions. Four stents were subjected to water at 37 °C at

typical ureteral flow rate and their mass was monitored weekly. After four weeks, data

could no longer be collected in the present study as the stent fractured and dissipated into

the flow apparatus. In this application, it is believed that this represents the time at which

the stent will break apart, flush into the bladder and then be expelled via urine. It should

be noted that this degradation time for the stent is much less than the typically reported

time of 6 months for PDO. [88], [89] This is because, in this application, the time of

strength loss of the PDO polymer equates to the time of stent fracture and migration into

the bladder. It has been reported that PDO suture typically suffers a drop in tensile strength of 65-90% after 4 weeks which aligns with our empirical data.

The mass of the stent was near consistent during the degradation study which provides evidence that the PDO stent was undergoing bulk degradation. In general, degrading polymers can erode in two ways. In surface erosion, the polymer degrades from the surface while in bulk erosion, degradation occurs throughout the whole material equally. As with nearly all polyesters, it has been shown that PDO undergoes bulk degradation. [90] This is due to the water diffusing into the polymer and then cleaving the ester bonds via hydrolysis. Hydrolytic degradation of ureteral stents in vivo would occur via an acid catalyzed process as the urinary tract is typically under acidic conditions (pH of 5.5-6.5 depending on diet). [84] This acid catalyzed degradation is essentially the reverse of Fischer Esterification where an acidic molecule penetrates the lamellar structure and cleaves the ester linkage. Degradation will depend on crystallinity and morphology. [91]. In the present study, degradation experiments were conducted in neutral deionized water (initial pH =7) with a regularly replaced reservoir used to dilute the acidic dioxanone polymer degradation products in the system. The main concern when conducting this study was if the stent would last too long, as in the majority of clinical cases, the stent is removed within 4 weeks. By performing the test under near neutral pH conditions, it is believed that the presented data represents an upper bound of stent degradation time and thus a worst case for stent implantation time.

The solution viscosity of a polymer is intrinsically tied to the molecular weight of a polymer. Essentially, the longer polymer chains are more prone to tangle in solution

and thus resist the fluid flow. The results of the solution viscosity testing provided evidence of a 12.7% decrease in viscosity after processing (Figure 4-10). Compared to the unprocessed suture (1.58±0.07 dL/g), the viscosity of the processed stent was 1.38±0.07 dL/g. The decrease in viscosity indicates that there is degradation occurring in the polymer during processing. The three primary methods of polymer degradation are chemical, thermal, and ultraviolet. Based on the DSC results (Figure 4.3), and the annealing process conditions, it is unlikely that the polymer experienced thermal or ultraviolet degradation. The most plausible explanation is that ambient moisture in the air provided enough initiator to start hydrolysis within the polymer. [92] Even though some degradation occurred in the stent during the annealing process, this may aid the final stent function as the stent will degrade in a shorter time which is more clinically relevant.

5.4 Physical Characterization of Stent

The presence of an ether peak (1320-1000), an ester peak (1750-1735), and the aldehyde group (2830-2695), indicated the expected structure of the PDO. The FTIR results verified that the polymer utilized to manufacture the stent was only PDO and was not contaminated by foreign substances during synthesis or sample preparation (Figure 4-7). The results of thermogravimetric analysis (TGA) revealed that both the processed and unprocessed stent reached 0% mass at 350 °C indicating the maximum molecular weight of both processed and unprocessed stents were the same. However, the graph also showed that processed stent started decreasing in mass at a lower temperature (Figure

4-2). This can be explained when molecular weight is viewed as a distribution of polymer chains. The data suggest that the unprocessed PDO polymer chains are uniform in length and, once temperature reached the sublimation temperature, they into the vapor phase simultaneously. In contrast, the processed stent exhibited an earlier deflection of the TGA curve at 200 °C compared to the unprocessed stent at 250 °C. This earlier sign of mass loss indicates that presence of smaller molecules that are easier to vaporize and removed from the polymer. This indicates degradation of the longer polymer chains into shorter ones during processing.

The primary aim in DSC testing was to determine the percent crystallinity of the polymers before and after processing. The enthalpy of fusion of a 100% crystalline polymer has been reported to be equal to 14400 J/mol. [93] Given a molar mass of 102 g/mol for PDO, this yields an enthalpy of melting of 141.12 J/g. The experimentally determined average enthalpy of fusion for the processed stent was 105.19 J/g while the unprocessed stent was measured to be 92.68 J/g. Dividing these values by the enthalpy of melting of 100% crystalline PDO yields a 74.50% crystallinity for processed stent samples and a 65.64% crystallinity for unprocessed suture. This gives an 8.86% increase in crystallinity due to processing.

This increase in crystallinity was further confirmed by the results of wide angle x-ray scattering (Figure 4-9). The intensity of the x-ray scatter showed a bimodal curve with an 8.9% increase in intensity in processed stents. Additionally, there is a slight shift of 0.26 degree in both the peaks toward a larger angle after processing the PDO suture into the stent. (Figure 4-9)

From the Bragg equation, ($2dsin\theta = \lambda$) given a 0.154 nm radiation wavelength, the lattice spacing of the suture was calculated to be 0.209 nm and 0.194 nm while the spacing for the stent was 0.207 nm and 0.192 nm. This decrease in lattice spacing is attributed to degradation of the polymer which was confirmed by IV testing. The cleaved polymer chains of the stent are shorter than the undegraded polymer chains of the suture. This allows the polymers to rest more closely to each other and slightly decreases the spacing between polymer chains.

The results of the DSC and WAXS data indicate there is an 8.9% increase in crystallinity during processing. PDO polymer typically exhibits a higher crystallinity than other degradable polymers such as PLA, one of the main reasons being lack of steric hindrance. This is also why PDO has a very low glass transition temperature of around -10 °C. [94] It can be speculated that this 8.9% increase in crystallinity is due to the added energy placed in the polymer from the 24 hours heat at 100 °C. This thermal energy allowed the amorphous polymer chains to move until they were in a more thermodynamically favorable position when the polymer is more crystalline. It is believed this crystallinity increase is the reason the annealed PDO is stiffer than the unannealed PDO. Thus, it is has been demonstrated that flexible, amorphous PDO can be formed into a spiral shape and "locked" into shape by annealing the material to increase its crystallinity.

6. CONCLUSION

In the present study, a biodegradable stent was designed and fabricated to solve many of the issues with current ureteral stents. These include, encrustation, urgency, pain, and most importantly the need for a follow up removal surgery. The proposed design features the use of biodegradable, FDA approved polydioxanone polymer material that was aimed to reduce encrustation and eliminate the need for a removal surgery. Additionally, the stent uses a coiled shape to anchor into the ureter, which will prevent the issue of the proximal anchor pressing on the bladder, remove the risk of encrustation on the distal anchor, and provide for better patient comfort by creating a more axially flexible stent. The results of the present study provided evidence that the stent exhibits adequate radial strength to maintain patency and can meet ureteral flow rate requirements. It was concluded that annealing PDO suture led to an increase in the polymer crystallinity and stiffness of the material. Moreover, an in vitro experiment demonstrated that the stent degrades in four weeks under physiological conditions, which is believed to be the ideal degradation time for the majority of ureteral stent applications.

7. FUTURE WORK

Future work should address the gaps in the stent characterization to ensure patient safety after implantation.

1. To determine the stent degradation profile, animal trials should be conducted to verify safety.

   Rationale: While stent degradation was studied in near physiological conditions in vitro, the degradation profile was not explored in vivo.

   Approach: A porcine animal model is typically used for a urinary system the stent should be monitored over the course of implantation using ultrasound or fluoroscopic techniques to track the stent degradation. Following implantation excretory urogram and blood tests would verify that adequate urine flow is occurring. After 5 weeks, all pigs should undergo necroscopy and undergo histological evaluation to verify no damage was done to the urinary tract during degradation.

2. A full sized stent and full sized sheath should be manufactured to verify efficacy of the implantation procedure.

Rationale: While implantation was proven feasible with approximately 4 cm stent segments, implantation was not attempted with a full sized stent.

Approach: Replacement of the tested silicone sheath with a material with a lower coefficient of friction will likely aid in implantation. One potential sheath material is Polytetrafluoroethylene (PTFE). This full sized stent should be implanted during the proposed animal study using standard urological techniques to verify implantation method.

3. An encrustation experiment using artificial urine should be conducted.

Rationale: it has been hypothesized that one of the benefits of utilizing a biodegradable stent is that it will reduce stent encrustation when compared to current stents on the market.

Approach: Encrustation could be quantified by measuring mass gain over time of a stent submersed in solution. Ideally, the typical stent materials of silicone and polyurethane would be tested under the same experimental conditions to compare the biodegradable material with current standards.

APPENDIX

Code for Pressure Vessel Used in Radial Strength Testing

```
#include <Wire.h>
#include <Adafruit_BMP085.h>

// Connect VCC of the BMP085 sensor to 3.3V (NOT 5.0V!)
// Connect GND to Ground
// Connect SCL to i2c clock - on '168/'328 Arduino Uno/Duemilanove/etc thats Analog 5
// Connect SDA to i2c data - on '168/'328 Arduino Uno/Duemilanove/etc thats Analog 4
// EOC is not used, it signifies an end of conversion
// XCLR is a reset pin, also not used here

Adafruit_BMP085 bmp;

void setup() {
  Serial.begin(115200);
  if (!bmp.begin()) {
        Serial.println("Could not find a valid BMP085 sensor, check wiring!");
        while (1) {}
  }
}

void loop() {


  //Serial.print("Pressure = ");
  Serial.print(bmp.readPressure());
  //Serial.println(" Pa");


  Serial.println();
  delay(100); //sampling every 100ms
}
```

REFERENCES

[1]   I. G. Jeong, K. S. Han, J. Y. Joung, H. K. Seo, and J. Chung, "The outcome with
        ureteric stents for managing non-urological malignant ureteric obstruction," *BJU
        Int.*, vol. 100, no. 6, pp. 1288–91, 2007.

[2]   M. Talja, T. Valima, T. Tammela, A. Petas, and P. Tormala, "Bioabsorbable and
        biodegradable stents in urology," *J. Endourol.*, vol. 11, no. 6, pp. 391–7, Dec.
        1997.

[3]   R. Miyaoka and M. Monga, "Ureteral stent discomfort: Etiology and
        management.," *Indian J. Urol.*, vol. 25, no. 4, pp. 455–60, 2009.

[4]   J.-S. Lim, C.-K. Sul, K.-H. Song, Y.-G. Na, J.-H. Shin, T.-H. Oh, and Y.-H. Kim,
        "Changes in urinary symptoms and tolerance due to long-term ureteral double-J
        stenting," *Int. Neurourol. J.*, vol. 14, no. 2, pp. 93–9, Aug. 2010.

[5]   G. Bithelis, N. Bouropoulos, E. N. Liatsikos, P. Perimenis, P. G. Koutsoukos, and
        G. A. Barbalias, "Assessment of encrustations on polyurethane ureteral stents," *J.
        Endourol.*, vol. 18, no. 6, pp. 550–6, Aug. 2004.

[6]   T. A. Wollin, C. Tieszer, J. V Riddell, J. D. Denstedt, and G. Reid, "Bacterial
        biofilm formation, encrustation, and antibiotic adsorption to ureteral stents
        indwelling in humans," *J. Endourol.*, vol. 12, no. 2, pp. 101–11, Apr. 1998.

[7]   S. L. Waters, K. Heaton, J. H. Siggers, R. Bayston, M. Bishop, L. J. Cummings, D.
        M. Grant, J. M. Oliver, and J. A. D. Wattis, "Ureteric stents: Investigating flow
        and encrustation," *Proc. Inst. Mech. Eng. Part H J. Eng. Med.*, vol. 222, no. 4, pp.
        551–561, Apr. 2008.

[8]   P. A. Cadieux, B. H. Chew, L. Nott, S. Seney, C. N. Elwood, G. R. Wignall, L. W.
        Goneau, and J. D. Denstedt, "Use of triclosan-eluting ureteral stents in patients
        with long-term stents," *J. Endourol.*, vol. 23, no. 7, pp. 1187–94, 2009.

[9]   UMHS Department of Urology, "Frequently Asked Questions about Ureteral
        Stents," *Hospital Publication*, 2007. [Online]. Available:
        https://www.med.umich.edu/1libr/urology/umureteral_stents.pdf.

[10]   E. Kehinde, V. Rotimi, A. Al-Hunayan, H. Abdul-Halim, F. Boland, and K. Al-
        Awadi, "Bacteriology of urinary tract infection associated with indwelling J
        ureteral stents," *J Endourol*, vol. 18, no. 9, pp. 891–6, 2004.

[11]   I. Peate, "Body fluids: Components and disorders of urine," *Br. J. Heal. Care
        Assist.*, vol. 02, no. 05, pp. 230–233, 2008.

[12] M. McKinley and V. O'Loughlin, *Human Anatomy*, 2nd ed. McGraw-Hill Companies, Incorporated, 2009.

[13] National Institutes of Health, "The Urinary Tract and How it Works," *NIH Publication No. 14–3195*, 2013. [Online]. Available: http://kidney.niddk.nih.gov/kudiseases/pubs/yoururinary/YourUrinary_508.pdf. [Accessed: 05-Jun-2013].

[14] National Institutes of Health, "The Kidneys and How They Work," *NIH Publication No. 14–3195*, 2014. [Online]. Available: http://www.niddk.nih.gov/health-information/health-topics/Anatomy/kidneys-how-they-work/Documents/yourkidneys_508.pdf. [Accessed: 05-Jun-2013].

[15] "Kidney," *Encyclopædia Britannica*, 2013. [Online]. Available: http://www.britannica.com/science/kidney. [Accessed: 05-Jun-2013].

[16] Y. Nakagawa, "Mechanical property of the human ureter," *Japanese J. Urol.*, vol. 80, no. 10, pp. 1481–1488, 1989.

[17] R. Fröber, "Surgical anatomy of the ureter," *BJU Int.*, vol. 100, no. 4, pp. 949–65, 2007.

[18] N. S. Schenkman, "Ureter Anatomy." [Online]. Available: http://emedicine.medscape.com/article/1949127-overview. [Accessed: 05-Jun-2013].

[19] P. Santicioli and C. A. Maggi, "Myogenic and neurogenic factors in the control of pyeloureteral motility and ureteral peristalsis," *Pharmacol. Rev.*, vol. 50, no. 4, pp. 683–721, 1998.

[20] M. Ordon, T. D. Schuler, D. Ghiculete, K. T. Pace, and R. J. J. D. Honey, "Stones lodge at 3 sites of anatomic narrowing in the ureter – Clinical fact or fiction?," *J. Endourol.*, vol. 27, no. 3, p. 120917133301000, 2012.

[21] W. Kahle, H. Leonhardt, and W. Platzer, *Color Atlas and Textbook of Human Anatomy*. Georg Thieme ; New York, 1993.

[22] X. Jiang, I. Luttrell, D. Y. Li, C. C. Yang, and K. Chitaley, "Altered bladder function in elastin-deficient mice at baseline and in response to partial bladder outlet obstruction," *BJU Int.*, vol. 110, no. 3, pp. 413–9, Aug. 2012.

[23] G. E. Lemack, Z. Szabo, Z. Urban, C. D. Boyd, K. Csiszar, E. D. Vaughan, and D. Felsen, "Altered bladder function in transgenic mice expressing rat elastin," *Neurourol. Urodyn.*, vol. 18, no. 1, pp. 55–68, Jan. 1999.

[24] B. Djavan, V. Lin, E. P. Kaplan, J. C. Richier, S. Shariat, M. Marberger, and J. D. McConnell, "Decreased elastin gene expression in noncompliant human bladder tissue: A competitive reverse transcriptase-polymerase chain reaction analysis," *J. Urol.*, vol. 160, no. 5, pp. 1658–1662, 1998.

[25] UCLA Department of Urology, "Vesicoureteral Reflux." [Online]. Available: http://urology.ucla.edu/body.cfm?id=478&ref=20&action=detail. [Accessed: 19-Jun-2013].

[26] IkramUllah, K. Alam, B. G. Wazir, F. Shah, A. Nawaz, and A. Malik, "Indications and morbidity of indwelling ureteral stenting," *Ann. Pakistan Inst. Med. Sci.*, vol. 7, no. 4, pp. 173–175, 2011.

[27] T. Kawahara, H. Ito, H. Terao, M. Yoshida, and J. Matsuzaki, "Ureteral stent encrustation, incrustation, and coloring: Morbidity related to indwelling times," *J. Endourol.*, vol. 26, no. 2, pp. 178–82, Feb. 2012.

[28] H. M. Rosevear, S. P. Kim, D. L. Wenzler, G. J. Faerber, W. W. Roberts, and J. S. Wolf Jr, "Retrograde ureteral stents for extrinsic ureteral obstruction: Nine years' experience at University of Michigan," *Urology*, vol. 70, no. 5, pp. 846–50, 2007.

[29] D. A. Bloom, R. V Clayman, and E. McDougal, "Stents and related terms: A brief history," *Urology*, vol. 54, no. 4, pp. 767–71, 1999.

[30] F. S. Howard and F. Hinman, "The ureteral splint in the repair of ureteropelvic avulsion," *J. Urol.*, vol. 68, no. 1, pp. 148–57, Jul. 1952.

[31] J. L. Marmar, "The management of ureteral obstruction with silicone rubber splint catheters," *J. Urol.*, vol. 104, no. 3, pp. 386–9, Sep. 1970.

[32] R. B. Dyer, M. Y. Chen, R. J. Zagoria, J. D. Regan, C. G. Hood, and P. V Kavanagh, "Complications of ureteral stent placement," *RadioGraphics*, vol. 22, no. 5, pp. 1005–1022, 2002.

[33] J. A. Tremann and T. L. Marchioro, "Gibbons ureteral stent in renal transplant recipients," *Urology*, vol. 9, no. 4, pp. 390–3, Apr. 1977.

[34] H. K. Mardis, T. W. Hepperlen, and H. Kammandel, "Double pigtail ureteral stent," *Urology*, vol. 14, no. 1, pp. 23–6, Jul. 1979.

[35] H. B. Joshi, A. Stainthorpe, R. P. MacDonagh, F. X. Keeley, A. G. Timoney, and M. J. Barry, "Indwelling ureteral stents: Evaluation of symptoms, quality of life and utility," *J. Urol.*, vol. 169, no. 3, pp. 1065–9; discussion 1069, Mar. 2003.

[36]   N. A. Memon, A. A. Talpur, and J. M. Memon, "Indications and complications of indwelling ureteral stenting at NMCH, Nawabshah," *Pakistan J. Surg.*, vol. 23, no. 3, pp. 187–191, 2007.

[37]   D. L. Wenzler, S. P. Kim, H. M. Rosevear, G. J. Faerber, W. W. Roberts, and J. S. Wolf Jr, "Success of ureteral stents for intrinsic ureteral obstruction," *J. Endourol.*, vol. 22, no. 2, pp. 295–9, Feb. 2008.

[38]   D. Bergqvist, H. Pärsson, and A. Sherif, "Arterio-ureteral fistula--A systematic review," *Eur. J. Vasc. Endovasc. Surg.*, vol. 22, no. 3, pp. 191–6, Sep. 2001.

[39]   N. Venkatesan, S. Shroff, K. Jayachandran, and M. Doble, "Polymers as ureteral stents," *J. Endourol.*, vol. 24, no. 2, pp. 191–8, 2010.

[40]   D. Tolley, "Ureteric stents, far from ideal," *Lancet*, vol. 356, no. 9233, pp. 872–3, Sep. 2000.

[41]   B. H. Chew, M. Duvdevani, and J. D. Denstedt, "New developments in ureteral stent design, materials and coatings," *Expert Rev. Med. Devices*, vol. 3, no. 3, pp. 395–403, Jun. 2006.

[42]   H. Razvi, J. C. Williams, A. P. Evan, J. E. Lingeman, and J. A. McAteer, "Ureteral Stent Coatings: What's Here and What's Coming," in *AIP Conference Proceedings*, 2008, vol. 1049, no. 1, pp. 182–185.

[43]   M. M. Tunney, P. F. Keane, D. S. Jones, and S. P. Gorman, "Comparative assessment of ureteral stent biomaterial encrustation," *Biomaterials*, vol. 17, no. 15, pp. 1541–1546, Aug. 1996.

[44]   N. Venkatesan, S. Shroff, K. Jeyachandran, and M. Doble, "Effect of uropathogens on in vitro encrustation of polyurethane double J ureteral stents," *Urol. Res.*, vol. 39, no. 1, pp. 29–37, Feb. 2011.

[45]   D. S. Jones, M. C. Bonner, S. P. Gorman, M. Akay, and P. F. Keane, "Sequential polyurethane-poly(methylmethacrylate) interpenetrating polymer networks as ureteral biomaterials: Mechanical properties and comparative resistance to urinary encrustation," *J. Mater. Sci. Mater. Med.*, vol. 8, no. 11, pp. 713–717, Nov. 1997.

[46]   R. M. Rabinow, B.E. Ding, Y.S. Qin, C. McHalsky, M.L. Schneider, J.H. Ashline, K.A. Shelbourn, T.L. Albrecht, B. Rabinow, Y. Ding, and C. Qin, "Biomaterials with permanent hydrophilic surfaces and low protein adsorption properties," *J. Biomater. Sci. Polym. Ed.*, vol. 6, no. 1, pp. 91–109, Jan. 1995.

[47] Society of Plastics Engineers Technical Conference, *ANTEC '96: Plastics--Racing Into the Future : Conference Proceedings, May 5-10, Indianapolis*. Society of Plastics Engineers, 1996.

[48] M. B. Chan-Park, A. Zhu, C. Sing Lim, and H. Chean Lim, "Argon-plasma-assisted graft polymerization of thick hydrogels with controllable water swelling on Chronoflex," *J. Adhes. Sci. Technol.*, vol. 18, no. 14, pp. 1663–1673, 2004.

[49] B. Silverstein, K. M. Witkin, V. H. Frankos, and A. I. Terr, "Assessing the role of the biomaterial Aquavene in patient reactions to Landmark midline catheters," *Regul. Toxicol. Pharmacol.*, vol. 25, no. 1, pp. 60–67, 1997.

[50] H. K. Mardis, R. M. Kroeger, J. J. Morton, and J. M. Donovan, "Comparative evaluation of materials used for internal ureteral stents," *J. Endourol.*, vol. 7, no. 2, pp. 105–15, 1993.

[51] P. K. Grover, R. L. Moritz, R. J. Simpson, and R. L. Ryall, "Inhibition of growth and aggregation of calcium oxalate crystals in vitro--A comparison of four human proteins," *Eur. J. Biochem.*, vol. 253, no. 3, pp. 637–644, 1998.

[52] S. K. Choong, S. Wood, and H. N. Whitfield, "A model to quantify encrustation on ureteric stents, urethral catheters and polymers intended for urological use," *BJU Int.*, vol. 86, no. 4, pp. 414–421, 2000.

[53] D. L. Nelson and M. M. Cox, *Lehninger Principles of Biochemistry*. New York: W H Freeman, 2008.

[54] C. R. Riedl, M. Witkowski, E. Plas, and H. Pflueger, "Heparin coating reduces encrustation of ureteral stents: A preliminary report," *Int. J. Antimicrob. Agents*, vol. 19, no. 6, pp. 507–510, Jun. 2002.

[55] J. M. Schierholz, U. T. Seyfert, A. F. E. Rump, J. Beuth, and G. Pulverer, "Strategies for the prevention of catheter material-associated thrombosis and bloodstream infections," *Transfus. Med. Hemotherapy*, vol. 26, no. 5, pp. 278–287, 1999.

[56] M. M. Tunney and S. P. Gorman, "Evaluation of a poly(vinyl pyrollidone)-coated biomaterial for urological use," *Biomaterials*, vol. 23, no. 23, pp. 4601–4608, 2002.

[57] A. D. Benson, E. R. Taylor, and B. F. Schwartz, "Metal ureteral stent for benign and malignant ureteral obstruction," *J. Urol.*, vol. 185, no. 6, pp. 2217–2222, 2011.

[58] H. L. López-Huertas, A. J. Polcari, A. Acosta-Miranda, and T. M. T. Turk, "Metallic ureteral stents: A cost-effective method of managing benign upper tract obstruction," *J. Endourol.*, vol. 24, no. 3, pp. 483–485, Mar. 2010.

[59] F. J. Trueba Arguiñarena and E. Fernández del Busto, "Self-expanding polytetrafluoroethylene covered nitinol stents for the treatment of ureteral stenosis: preliminary report," *J. Urol.*, vol. 172, no. 2, pp. 620–3, 2004.

[60] S. Laaksovirta, T. Välimaa, T. Isotalo, P. Törmälä, M. Talja, and T. L. J. Tammela, "Encrustation and strength retention properties of the self-expandable, biodegradable, self-reinforced L-lactide-glycolic acid co-polymer 80:20 spiral urethral stent in vitro," *J. Urol.*, vol. 170, no. 2 pt 1, pp. 468–71, 2003.

[61] Y. S. Song, J. T. Lee, and J. R. Youn, "Natural fiber reinforced PLA composites," in *AIP Conference Proceedings*, 2010, vol. 1255, no. 1, pp. 261–263.

[62] D. Chen, J. Li, and J. Ren, "Crystal and thermal properties of PLLA/PDLA blends synthesized by direct melt polycondensation," *J. Polym. Environ.*, vol. 19, no. 3, pp. 574–581, 2011.

[63] J. Lumiaho, A. Heino, S. Aaltomaa, T. Välimaa, and M. Talja, "A short biodegradable helical spiral ureteric stent provides better antireflux and drainage properties than a double-J stent," *Scand. J. Urol. Nephrol.*, vol. 45, no. 2, pp. 129–33, 2011.

[64] J. Lumiaho, A. Heino, T. Kauppinen, M. Talja, E. Alhava, T. Välimaa, and P. Törmälä, "Drainage and antireflux characteristics of a biodegradable self-reinforced, self-expanding X-ray-positive poly-L,D-lactide spiral partial ureteral stent: An experimental study," *J. Endourol.*, vol. 21, no. 12, pp. 1559–64, 2007.

[65] G. Li, Z. X. Wang, W. J. Fu, B. F. Hong, X. X. Wang, L. Cao, F. Q. Xu, Q. Song, F. Z. Cui, and X. Zhang, "Introduction to biodegradable polylactic acid ureteral stent application for treatment of ureteral war injury," *BJU Int.*, vol. 108, no. 6, pp. 901–906, 2011.

[66] J. E. Lingeman, G. M. Preminger, Y. Berger, J. D. Denstedt, L. Goldstone, J. W. Segura, B. K. Auge, J. D. Watterson, and R. L. Kuo, "Use of a temporary ureteral drainage stent after uncomplicated ureteroscopy: results from a phase II clinical trial," *J. Urol.*, vol. 169, no. 5, pp. 1682–8, 2003.

[67] D. Lange and B. H. Chew, "Update on ureteral stent technology," *Ther. Adv. Urol.*, vol. 1, no. 3, pp. 143–8, 2009.

[68] Dulcera Market Analysis, "Ureteral Stent - Market Analysis," 2011.

[69] Cook Medical, "Temporary Ureteral Stent Placement or Removal 2013 Coding and Reimbursement Guide," 2013.

[70] E. Aravantinos, S. Gravas, A. D. Karatzas, V. Tzortzis, and M. Melekos, "Forgotten, encrusted ureteral stents: A challenging problem with an endourologic solution," *J. Endourol.*, vol. 20, no. 12, pp. 1045–9, Dec. 2006.

[71] C. Xu, H. Tang, X. Gao, X. Gao, B. Yang, and Y. Sun, "Management of forgotten ureteral stents with holmium laser," *Lasers Med. Sci.*, vol. 24, pp. 140–143, 2009.

[72] M. Aron, M. S. ANSARI, I. Singh, G. Gautam, S. B. Kolla, A. Seth, and N. P. Gupta, "Forgotten ureteral stents causing renal failure: Multimodal endourologic treatment," *J. Endourol.*, vol. 20, no. 6, pp. 423–428, Jun. 2006.

[73] J. Djokic, "Development and characterisation of polycaprolactone as a biodegradable material for use in urinary tract devices," Queen's University of Belfast (United Kingdom), 1999.

[74] A. Brauers, H. Thissen, O. Pfannschmidt, H. Bienert, A. Foerster, D. Klee, W. Michaeli, H. Höcker, and G. Jakse, "Development of a biodegradable ureteric stent: Surface modification and in vitro assessment," *J. Endourol.*, vol. 11, no. 6, pp. 399–403, Dec. 1997.

[75] E. D. Boland, B. D. Coleman, C. P. Barnes, D. G. Simpson, G. E. Wnek, and G. L. Bowlin, "Electrospinning polydioxanone for biomedical applications," *Acta Biomater.*, vol. 1, no. 1, pp. 115–123, 2005.

[76] R. S. Bezwada, D. D. Jamiolkowski, I.-Y. Lee, V. Agarwal, J. Persivale, S. Trenka-Benthin, M. Erneta, J. Suryadevara, A. Yang, and S. Liu, "Monocryl suture, a new ultra-pliable absorbable monofilament suture," *Biomaterials*, vol. 16, no. 15, pp. 1141–1148, 1995.

[77] M. Zilberman, K. D. Nelson, and R. C. Eberhart, "Mechanical properties and in vitro degradation of bioresorbable fibers and expandable fiber-based stents," *J. Biomed. Mater. Res. - Part B Appl. Biomater.*, vol. 74, no. 2, pp. 792–799, 2005.

[78] M. J. Smith, M. J. McClure, S. A. Sell, C. P. Barnes, B. H. Walpoth, D. G. Simpson, and G. L. Bowlin, "Suture-reinforced electrospun polydioxanone-elastin small-diameter tubes for use in vascular tissue engineering: A feasibility study," *Acta Biomater.*, vol. 4, no. 1, pp. 58–66, Jan. 2008.

[79] G. Wypych, "Handbook of Polymers - Polydioxanone." ChemTec Publishing, p. 333, 2012.

[80] M. G. S. Andrade, R. Weissman, and S. R. A. Reis, "Tissue reaction and surface morphology of absorbable sutures after in vivo exposure," *J. Mater. Sci. Mater. Med.*, vol. 17, pp. 949–961, 2006.

[81] C. Ping Ooi and R. E. Cameron, "The hydrolytic degradation of polydioxanone (PDSII) sutures. Part I: Morphological aspects.," *J. Biomed. Mater. Res.*, vol. 63, no. 3, pp. 280–90, Jan. 2002.

[82] B. H. Chew, B. E. Knudsen, L. Nott, S. E. Pautler, H. Razvi, J. Amann, and J. D. Denstedt, "Pilot study of ureteral movement in stented patients: First step in understanding dynamic ureteral anatomy to improve stent comfort," *J. Endourol.*, vol. 21, no. 9, pp. 1069–75, Sep. 2007.

[83] E. Piorkowska and G. C. Rutledge, *Handbook of Polymer Crystallization*. Wiley, 2013.

[84] ASTM International, "ASTM F 1828-97 Standard Specification for Ureteral Stents," West Conshohocken, PA, 2006.

[85] J. D. Denstedt, "Advances in ureteral stent design.," *AIP Conf. Proc.*, pp. 272–277, May 2007.

[86] D. J. Griffiths, "Flow of urine through the ureter: a collapsible, muscular tube undergoing peristalsis.," *J. Biomech. Eng.*, vol. 111, no. 3, pp. 206–211, 1989.

[87] K. Hendlin, K. Dockendorf, C. Horn, N. Pshon, B. Lund, and M. Monga, "Ureteral stents: coil strength and durometer.," *Urology*, vol. 68, no. 1, pp. 42–5, Jul. 2006.

[88] Ethicon, "Ethicon Wound Closure Manual," Somerville, NJ, 2004.

[89] A. C. Vieira, J. C. Vieira, R. M. Guedes, and A. T. Marques, "Experimental degradation characterization of PLA-PCL, PGA-PCL, PDO and PGA fibres," in *17th International Conference on Composite Materials*, 2009.

[90] A. L. Sisson, M. Schroeter, and A. Lendlein, "Polyesters," *Handb. Biodegrad. Polym. Synth. Charact. Appl.*, pp. 1–21, 2011.

[91] M. A. Sabino, J. L. Feijoo, and A. J. Muller, "Crystallisation and morphology of poly(p-dioxanone)," *Macromol. Chem. Phys.*, vol. 201, no. 18, pp. 2687–2698, 2000.

[92] N. M. Emanuel and A. L. Buchachenko, *Chemical Physics of Polymer Degradation And Stabilization*. Utrecht, The Netherlands: VNU Science Press, 1987.

[93] K. Ishikiriyama, "Heat capacity of Poly-p-dioxanone," *J. Macromol. Sci.*, vol. 107, no. Table 111, pp. 27–44, 1998.

[94] P. Zamiri, Y. Kuang, U. Sharma, T. F. Ng, R. H. Busold, A. P. Rago, L. A. Core, and M. Palasis, "The biocompatibility of rapidly degrading polymeric stents in porcine carotid arteries," *Biomaterials*, vol. 31, pp. 7847–7855, 2010.